



Deciphering the molecular profile of plaques, memory decline and neuron loss in two mouse models for Alzheimer's disease by deep sequencing

Yvonne Bouter^{1†}, Tim Kacprowski^{2,3†}, Robert Weissmann⁴, Katharina Dietrich¹, Henning Borgers¹, Andreas Brauß¹, Christian Sperling⁴, Oliver Wirths¹, Mario Albrecht^{2,5}, Lars R. Jensen⁴, Andreas W. Kuss^{4*} and Thomas A. Bayer^{1*}

¹ Division of Molecular Psychiatry, Georg-August-University Goettingen, University Medicine Goettingen, Goettingen, Germany

² Department of Bioinformatics, Institute of Biometrics and Medical Informatics, University Medicine Greifswald, Greifswald, Germany

³ Department of Functional Genomics, Interfaculty Institute for Genetics and Functional Genomics, University Medicine Greifswald, Greifswald, Germany

⁴ Human Molecular Genetics, Department for Human Genetics of the Institute for Genetics and Functional Genomics, Institute for Human Genetics, University Medicine Greifswald, Ernst-Moritz-Arndt University Greifswald, Greifswald, Germany

⁵ Institute for Knowledge Discovery, Graz University of Technology, Graz, Austria

Edited by:

Isidro Ferrer, University of Barcelona, Spain

Reviewed by:

Isidro Ferrer, University of Barcelona, Spain

Dietmar R. Thal, University of Ulm, Germany

*Correspondence:

Andreas W. Kuss, Human Molecular Genetics, Department for Human Genetics of the Institute for Genetics and Functional Genomics, Institute for Human Genetics, University Medicine Greifswald, Ernst-Moritz-Arndt University Greifswald, Fleischmannstr. 42-44, Greifswald 17475, Germany

e-mail: kussa@uni-greifswald.de;

Thomas A. Bayer, Division of Molecular Psychiatry, Department of Psychiatry, Georg-August-University Goettingen, University Medicine Goettingen, von-Siebold-Strasse 5, Goettingen 37075, Germany
e-mail: tbayer@gwdg.de

[†]Yvonne Bouter and Tim Kacprowski have contributed equally to this work.

One of the central research questions on the etiology of Alzheimer's disease (AD) is the elucidation of the molecular signatures triggered by the amyloid cascade of pathological events. Next-generation sequencing allows the identification of genes involved in disease processes in an unbiased manner. We have combined this technique with the analysis of two AD mouse models: (1) The 5XFAD model develops early plaque formation, intraneuronal A β aggregation, neuron loss, and behavioral deficits. (2) The Tg4–42 model expresses N-truncated A β _{4–42} and develops neuron loss and behavioral deficits albeit without plaque formation. Our results show that learning and memory deficits in the Morris water maze and fear conditioning tasks in Tg4–42 mice at 12 months of age are similar to the deficits in 5XFAD animals. This suggested that comparative gene expression analysis between the models would allow the dissection of plaque-related and -unrelated disease relevant factors. Using deep sequencing differentially expressed genes (DEGs) were identified and subsequently verified by quantitative PCR. Nineteen DEGs were identified in pre-symptomatic young 5XFAD mice, and none in young Tg4–42 mice. In the aged cohort, 131 DEGs were found in 5XFAD and 56 DEGs in Tg4–42 mice. Many of the DEGs specific to the 5XFAD model belong to neuroinflammatory processes typically associated with plaques. Interestingly, 36 DEGs were identified in both mouse models indicating common disease pathways associated with behavioral deficits and neuron loss.

Keywords: fear conditioning, spatial reference memory, transcriptome, 5xHAD, Tg4–42, N-truncated abeta, Morris water maze, deep sequencing

INTRODUCTION

Alzheimer disease (AD) is the most common form of dementia in the aging population accounting for 60–80% of the cases. The disease is a progressive neurodegenerative disorder characterized by the presence of extracellular amyloid plaques composed of amyloid- β (A β) surrounded by dystrophic neurites and neurofibrillary tangles (NFT) (Alzheimer's Association, 2012). Further pathological hallmarks of the disease include inflammatory processes, synaptic and neuronal loss, cerebral atrophy, and cerebral amyloid angiopathy (CAA) (Wirths and Bayer, 2012). The complex progression of neurodegeneration in AD patients results in memory impairment and decline in other cognitive abilities often combined with non-cognitive symptoms like mood- and personality changes (Alzheimer's Association, 2012).

The discovery that certain early-onset familial forms of AD may be caused by an enhanced level of A β peptides led to the hypothesis that amyloidogenic A β is closely involved in the AD pathogenic process (Selkoe, 1998). The “amyloid hypothesis” that was proposed more than two decades ago claims that extracellular A β is the major elicitor of the disease (Hardy and Allsop, 1991). However, while the insoluble fibrillar aggregates of amyloid- β are the main neuropathological hallmark of AD, the plaque load correlates poorly with brain dysfunction and cognitive impairment in AD patients (Price and Morris, 1999; Lesné et al., 2013) or in AD transgenic mouse models (Moechars et al., 1999; Schmitz et al., 2004). In contrast, recent studies indicate that soluble A β levels, including soluble oligomers, correlate much better with key features of AD (McLean et al., 1999; Näslund et al., 2000; Selkoe, 2011).

There is increasing evidence that AD is primarily initiated by soluble oligomeric species derived from full-length $A\beta_{1-42}$ (Haass and Selkoe, 2007; Haupt et al., 2012). In addition to soluble oligomers, β -sheet containing amyloid fibrils are also highly toxic forms of $A\beta$ (Klein, 2002). Numerous variants of $A\beta_{1-42}$ oligomers including dimers, trimers, and tetramers have been introduced and are currently discussed as major factors in AD (Roychaudhuri et al., 2009; Benilova et al., 2012). The “modified amyloid hypothesis” now suggests that intraneuronal $A\beta$ accumulation precedes the formation of extracellular plaques and other pathological events in the brains of AD patients (Wirhth et al., 2004).

Next to the numerous variants of $A\beta_{1-42}$ oligomers there is substantial evidence that N-terminal truncated peptides play a key role in AD (Jawhar et al., 2011). Besides $A\beta$ peptides starting with an aspartate at position 1, a variety of different N-truncated $A\beta$ peptides have been identified in AD brains. Ragged $A\beta$ peptides, including a major species beginning with phenylalanine at position 4 of $A\beta$ ($A\beta_{4-42}$), have been reported as early as 1985 by Masters et al. (1985).

Only a subgroup of patient families displays the early-onset familial form of AD that is caused by rare single mutations in either the amyloid-protein-precursor (APP) or the presenilin-1 (PSEN-1) and presenilin 2 (PSEN-2) genes. The vast majority of AD patients displays no known mutations and suffers from the sporadic late-onset form of AD (Blennow et al., 2006). To date, the apolipoprotein E (ApoE) $\epsilon 4$ allele is the only known genetic risk factor for sporadic AD (Blennow et al., 2006; Selwood et al., 2009). A variety of additional genetic loci have been proposed to be involved with late-onset AD (Bertram and Tanzi, 2001).

Technical approaches using transcriptome microarray analyses were performed over the last years to identify genes that are differentially expressed and therefore may be involved in the pathophysiology of AD (George et al., 2010).

The recent developments in next-generation sequencing (deep sequencing) offer a more comprehensive and most of all unbiased approach for transcriptome analysis. Multiple studies already indicate that next-generation sequencing is more useful and particularly suitable to investigate the pathogenesis of complex neurodegenerative diseases like AD (Twine et al., 2011). For example, Sultan et al. (2008) claimed that deep sequencing of non-ribosomal RNA (RNA-Seq) could detect up to 25% more genes compared to microarrays analyses.

In the present study, we performed a comparative gene expression analysis of brain tissue of two different mouse models for AD using next-generation sequencing. We compared the well-established, plaque-developing 5XFAD mouse model (Oakley et al., 2006) with the Tg4–42 mouse model that solely expresses $A\beta_{4-42}$ without extracellular plaque deposition (Bouter et al., 2013). The aim of this study was to elucidate the similarities and distinctions in expression profiles of these two mouse models that display similar memory deficits.

MATERIALS AND METHODS

TRANSGENIC MICE

In this study, we used the transgenic mouse lines Tg4–42 and 5XFAD. The generation of Tg4–42 has been recently described by our lab (Bouter et al., 2013). Tg4–42 mice express human $A\beta_{4-42}$

fused to the murine TRH signal peptide under the control of the neuronal Thy-1 promoter.

5XFAD mice over-express the 695 amino acids isoform of the human amyloid precursor protein (APP695) carrying the Swedish, London, and Florida mutations under the control of the murine Thy-1 promoter. In addition, human presenilin-1 (PSEN-1) carrying the M146L/L286V mutations is expressed also under the control of the murine Thy-1 promoter (Oakley et al., 2006). 5XFAD mice used in the current study were backcrossed for more than eight generations to C57Bl/6J wildtype mice (Jackson Laboratories, Bar Harbor, ME, USA) to obtain an incipient congenic line on a C57Bl/6J genetic background (Jawhar et al., 2010). Young (3–6 months) and aged (12 months) Tg4–42, 5XFAD mice, and wildtype (WT, C57Bl/6J) controls were tested. In the current study, only female mice were used. Wildtype littermate control mice served as age-matched control animals. All animals were handled according to the German guidelines for animal care. All efforts were made to minimize suffering and the number of animals used for this study.

SPATIAL REFERENCE MEMORY BY MORRIS WATER MAZE

Spatial reference memory in Tg4–42 and 5XFAD mice was evaluated using the Morris water maze (Morris, 1984) as described previously (Bouter et al., 2013). In brief, mice learn to use spatial cues to locate a hidden platform in a circular pool filled with opaque water. The pool was divided into four virtual quadrants that were defined based on their spatial relationship to the platform: left, right, opposite, and target quadrant, which contains the goal platform. ANY-Maze video tracking software (Stoelting Co., Wood Dale, IL, USA) was used to record escape latency, swimming speed, and quadrant preference.

Young and aged Tg4–42, 5XFAD mice, and wildtype (WT, C57Bl/6J) controls were tested ($n = 8-11$ mice per group).

The experiment began with 3 days of cued training during which the platform was marked with a triangular flag. Both the location of the platform and the position where mice were introduced into the pool changed between trials. Each mouse received four training trials per day with an average inter-trial interval of 15 min.

Twenty-four hours after the last day of cued training, mice performed 5 days of acquisition training. For this part of testing, the flag was removed from the platform. In addition to the distal cues existing in the room, proximal visual cues were attached to the outside of the pool. The platform location remained stationary for each mouse throughout training. Trials were conducted as during the cued training phase.

Twenty-four hours after the last acquisition trial, a probe test was performed to assess spatial reference memory. The platform was removed from the pool, and mice were introduced into the water from a novel entry point. Mice were then allowed to swim freely for 1 min while their swimming path was recorded. After the probe trial, the mice were sacrificed.

CONTEXTUAL AND TONE FEAR CONDITIONING

Twelve-month-old Tg4–42, 5XFAD, and WT mice were subjected to contextual fear conditioning (CFC) and tone fear conditioning (TFC) ($n = 11-13$). A 3-day delay fear conditioning protocol

was used to assess conditional learning and memory. According to this protocol, the *conditioned stimulus* (CS) is presented and overlapped by the presentation of the *unconditioned stimulus* (US) (Ohno, 2009).

The experiments were performed using a standard conditioning chamber (17 cm × 17 cm × 26 cm) with a stainless steel grid floor connected to a shock generator (Ugo Basile Sound and Shocker Generator, Comerio, Italy). The walls were covered with black and white checkered paper (CS). The chamber was housed in a soundproof isolation cubicle. A digital camera and an additional light source were attached to the ceiling of the cubicle. ANY-Maze video tracking software (Stoelting Co., Wood Dale, IL, USA) was used to record freezing behavior of animals.

On day one, mice were placed in the conditioning chamber and allowed to explore the box for 150 s. After the habituation period, a tone (2000 Hz, 80 dB; CS) was presented for 30 s that simultaneously ended with a 2 s foot-shock (0.7 mA, US). Mice were allowed to recover after the foot-shock for an additional 30 s before being returned to their home cage. Baseline freezing was recorded before the presentation of the tone.

Twenty-four hours after the training mice were placed back in the familiar fear conditioning chamber, but in the absence of tones and foot-shocks. Freezing behavior was measured for 210 s to test contextual memory retrieval.

For the tone fear retrieval trial on day 3, mice were placed for 3 min in an altered conditioning chamber with white walls, a covered floor, and an acetic acid scent. After 150 s baseline recording, a tone similar to the one used during the fear conditioning trial was presented for 30 s. The freezing behavior before and during the CS tone was measured. Mice were sacrificed after the tone trial.

STATISTICAL ANALYSIS OF BEHAVIOR EXPERIMENTS

Differences between groups were tested with unpaired *t*-test, one-way analysis of variance (ANOVA) followed by Bonferroni multiple comparisons or repeated measures ANOVA followed by Bonferroni multiple comparisons as indicated. All data are given as means ± standard error of the mean (SEM). Significance levels are given as follows: ****p* < 0.001; ***p* < 0.01; **p* < 0.05. All statistics were calculated using STATISTICA version 10.0 for Windows (StatSoft, Tulsa, OK, USA) and GraphPad Prism version 5.04 for Windows (GraphPad Software, San Diego, CA, USA).

TISSUE HARVESTING

Mice were sacrificed via CO₂ anesthetization followed by cervical dislocation. Brain hemispheres were carefully dissected (olfactory bulbs and cerebellum was removed), frozen on dry-ice and stored at −80°C for subsequent use.

RNA EXPRESSION PROFILING

Expression profiling for young and aged Tg4–42, 5XFAD, and WT mice was performed by next-generation sequencing on a SOLiD 5500xl Genetic Analyzer (Life Technologies, Carlsbad, CA, USA). RNA was extracted from mouse brain hemispheres as follows. The tissue was homogenized using a Polytron (VWR) device and then treated with TRIzol (Life Technologies, Carlsbad, CA, USA). Next, 5 μg of each total RNA sample were spiked with ERCC spike-in control mixes (Life Technologies, Carlsbad, CA, USA)

before removal of the rRNA by use of a RiboZero Kit (Epicentre, Madison, WI, USA). The RNA was prepared for sequencing following the protocol provided by the manufacturer of the sequencer. In brief, the rRNA depleted RNA was fragmented by chemical hydrolysis, phosphorylated, and purified. Adaptors were ligated to the RNA fragments, which subsequently were reverse transcribed into cDNA. The cDNA was purified and size-selected using two rounds of Agencourt AMPure XP bead purification (Beckman Coulter Genomics, Danvers, MA, USA) and released from the beads. The sample was amplified by 12 PCR cycles in the presence of primers that contained unique sequences (barcoding). The size distribution and concentration of the fragments were determined with an Agilent 2100 Bioanalyzer and the corresponding chemicals (Agilent Technologies, Santa Clara, CA, USA).

The cDNA fragments were pooled in equimolar amounts and diluted to 76 pg/μL corresponding to a concentration of 500 pM. Fifty microliters of this dilution was mixed with a freshly prepared oil emulsion, P1 and P2 reagents, and P1 beads in a SOLiD EZ Bead Emulsifier prepared according to the E80 scale protocol (Life Technologies, Carlsbad, CA, USA). The emulsion PCR was carried out in a SOLiD EZ Bead Amplifier (Life Technologies, Carlsbad, CA, USA) using the E80 setting. To enrich for the beads that carried amplified template DNA, the beads were purified on a SOLiD EZ Bead Enricher using the recommended chemicals and software (Life Technologies, Carlsbad, CA, USA). The purified beads were loaded onto a SOLiD 6-lane Flowchip and incubated upside down for 1 h at 37°C. The Flowchip was positioned in the 5500xl SOLiD System and the DNA was sequenced using the settings and recommended chemicals for sequencing 75 nucleotides in the forward direction and 35 nucleotides in the reverse direction (Life Technologies, Carlsbad, CA, USA).

Sequence reads were mapped to the mouse genome reference sequence mm10¹ using the workflow “whole.transcriptome.pe” LifeScope-v2.5.1-r0 (Life Technologies, Carlsbad, CA, USA). Reads mapping to RefSeq coding exons (accessed 2012-06-27)² and matching the coding strand were considered as coding RNAs. All other mapping reads were considered non-coding.

DIFFERENTIAL EXPRESSION ANALYSIS

RNA-Seq read data were normalized within and between lanes for GC-content using EDASeq’s full-quantile normalization (Risso et al., 2011). The differential expression analysis was done with DESeq (Anders and Huber, 2010). All samples were treated as replicates of a single condition for the estimation of the dispersion. Only the fitted dispersion values were used in the following analyses. The significance of differential expression was determined by the Benjamini–Hochberg corrected *p*-values of the negative binomial test between two conditions. The threshold for significance was set to *p* = 0.05. The following conditions were compared: young WT vs. young Tg4–42, young WT vs. young 5XFAD, aged WT vs. aged Tg4–42, and aged WT vs. aged 5XFAD. Genes with more than 200 reads were successfully verified by real-time quantitative PCR (qRT-PCR) and are listed in the results part. Genes with an expression level lower than 200 reads are not shown.

¹ <http://hgdownload.cse.ucsc.edu/goldenPath/mm10/>

² <http://hgdownload.cse.ucsc.edu/goldenPath/mm10/database/refGene.txt.gz>

REAL-TIME QUANTITATIVE PCR CONFIRMATION

RNA was isolated from female young and aged 5XFAD mice, aged Tg4–42, and aged-matched WT mice ($n = 5$ each) as described previously (Hillmann et al., 2012). Briefly, frozen right brain hemispheres were homogenized with 10 strokes of a R50D homogenizer (CAT) set at 800 rpm in 1.5 mL ice-cold Trifast® (Peqlab, Erlangen, Germany). Three hundred microliters chloroform (Merck) was added to each sample. After 10 min incubation, the samples were centrifuged at $12000 \times g$ for 15 min at 4°C to separate the RNA. The upper RNA-containing aqueous phase was transferred into a new tube, vigorously mixed with 500 μ L Isopropanol, and incubated for 20 min on ice. After centrifugation at $12000 \times g$ for 10 min at 4°C, the supernatant was discarded. RNA pellets were washed twice with 500 μ L 75% Ethanol. After the pellet was air-dried, the RNA was dissolved in 30 μ L of RNase free water. RNA was stored at -80°C until further use. RNA purity and yields were determined by a Biophotometer (Eppendorf, Hamburg, Germany).

Total RNA (1 μ g) was subjected to reverse transcription to synthesize cDNA using the First-Strand cDNA Synthesis Kit (Fermentas, St. Leon-Rot, Germany) according to the manufacturer's instructions. Prior to reverse transcription, RNA was subjected to digestion by DNase using a DNase Digestion Kit (Fermentas, St. Leon-Rot, Germany). Generated cDNA was diluted 1:10 in ddH₂O and used as the sample template for qRT-PCR. The obtained cDNA was stored at -20°C until use.

Quantitative PCR was used to validate the results obtained from the deep sequencing analysis. Several genes were selected for both transgenic mouse lines and time points. Primers were purchased from Eurofins (Ebersberg, Germany) as intron-spanning validated primer pairs. The diluted first-strand cDNA was used for qRT-PCR using the SYBR green based DyNAmo Flash SYBR Green qPCR Kit (Thermo Fischer Scientific, Waltham, MA, USA) containing ROX as an internal reference dye. Samples were normalized to the housekeeping gene β -Actin.

Analysis of brain transgene expression in 5XFAD, Tg4–42, and WT animals was performed in the MX3000P Real-Time Cyclor (Stratagene, Santa Clara, CA, USA) and data collected using the MxPro Mx3000P software (Stratagene, Santa Clara, CA, USA). Statistical analysis of quantitative RT-PCR measurements was done using the Relative Expression Software Tool V1.9.6 (REST, Qiagen, Hilden, Germany) (Pfaffl et al., 2002). The expression ratio results of the studied transcripts were tested for significance by Pair Wise Fixed Reallocation Randomization Test. *** $p < 0.001$; ** $p < 0.01$; * $p < 0.05$.

ANNOTATION ANALYSIS

In order to gain insight in the biological function and to understand the biological significance of differentially expressed genes (DEGs), the functional annotation of DEGs was obtained using Source³, GeneCards⁴, Wiki-Pi⁵, and Mouse Genome Informatics⁶.

³ <http://puma.princeton.edu/cgi-bin/source/sourceResult>

⁴ <http://www.genecards.org>

⁵ <http://severus.dbmi.pitt.edu/wiki-pi/index.php>

⁶ <http://www.informatics.jax.org/>

RESULTS

Tg4–42 AND 5XFAD MICE DISPLAY SPATIAL MEMORY DEFICITS

Spatial reference memory was assessed in Tg4–42, 5XFAD, and WT mice using the Morris water maze. First, mice performed cued training with a marked platform to familiarize with the pool and to rule out effects from possible motor or sensory deficits. WT, Tg4–42, and 5XFAD mice showed progressively decreased escape latencies at all ages tested and no differences in swimming speed (data not shown). The cued training revealed that all mice had an intact vision and appropriate motor abilities to swim.

Twenty-four hours after the cued training, mice were subjected to acquisition training in order to test their learning abilities to find the location of a submerged platform using distal and proximal cues.

We found a significant main effect of *genotype* for escape latencies (Repeated measures ANOVA, $F = 3.4097$; $p = 0.04$). Young Tg4–42, 5XFAD, and WT mice showed a significant decrease in the escape latencies to reach the hidden platform (Figure 1A, Repeated measures ANOVA, escape latency: $p = 0.000011$). Moreover, aged WT animals showed a significant decrease in the escape latencies while the escape latencies for aged Tg4–42 and 5XFAD did not improve over the 5 days of training (Figure 1B, Repeated measures ANOVA, escape latency: $p = 0.001$).

In contrast, the swimming speed across the 5 days of acquisition training showed no significant difference irrespective of genotype and age (Figures 1A,B, Repeated measures ANOVA, $p = 0.0566$).

Young Tg4–42 and 5XFAD animals performed superior to older animals while this difference was not due to differences in swimming velocity due to age-related motor deficits. These results suggest that spatial learning is impaired in aged Tg4–42 and 5XFAD mice.

Twenty-four hours after the last acquisition trial, a probe trial was given to assess spatial reference memory. Young Tg4–42, 5XFAD, and WT mice displayed a significant preference for the target quadrant, as indicated by the percentage time spent in different quadrants of the pool (Figure 2A, One-way ANOVA, WT: $p < 0.0001$, $df = 3$; $p < 0.001$ target vs. all other quadrants; 5XFAD: $p < 0.0001$, $df = 3$; $p < 0.001$ target vs. left and opposite quadrant, $p < 0.01$ target vs. right quadrant; Tg4–42: $p < 0.0001$, $df = 3$; $p < 0.001$ target vs. opposite quadrant, $p < 0.01$ target vs. right quadrant).

No quadrant preference was found for aged Tg4–42 and 5XFAD mice, while WT mice still demonstrated significant preference for the target quadrant at that time point (Figure 2B, One-way ANOVA, WT: $p < 0.0001$, $df = 3$; $p < 0.001$ target vs. left and opposite quadrant, $p < 0.01$ target vs. right quadrant). Swimming speed between the groups did not differ during the probe trial. The absence of a preference for the target quadrant as compared to the remaining quadrants during the probe trial demonstrates that aged Tg4–42 and 5XFAD mice display a robust deficit in spatial reference memory.

In summary, the results of the acquisition phase and the probe trial suggest that aged Tg4–42 and 5XFAD mice display an impaired spatial and spatial reference memory.

Tg4–42 AND 5XFAD MICE EXHIBIT DECREASED CONTEXTUAL LEARNING

During the initial training sessions involving tone-foot-shock pairing (CS/US), 12-month-old Tg4–42, 5XFAD, and WT mice

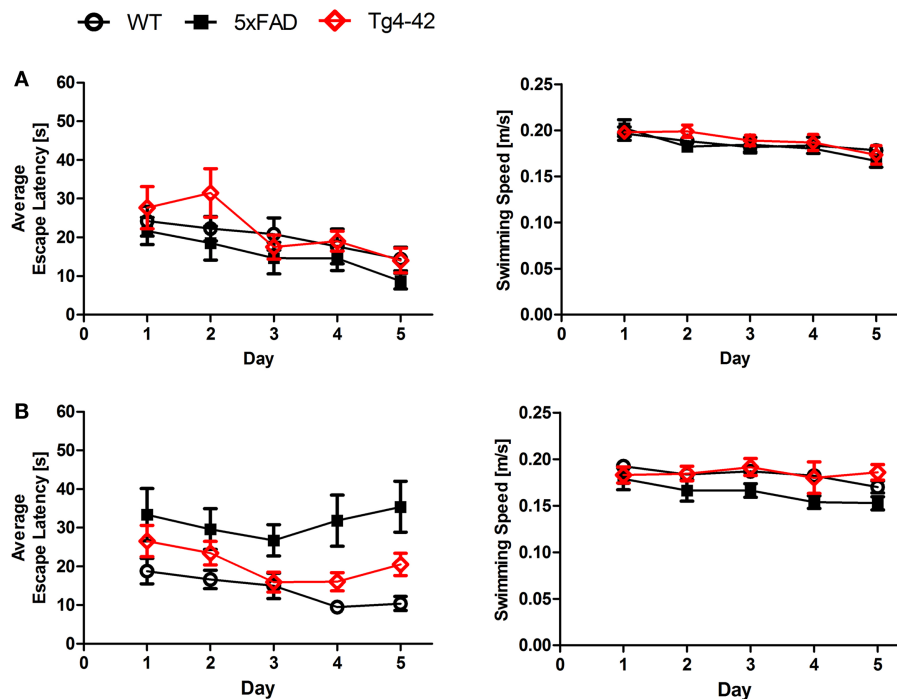


FIGURE 1 | Spatial learning deficits in aged Tg4-42 and 5XFAD shown in the acquisition training of the Morris water maze. Female (A) young and (B) aged Tg4-42 mice, 5XFAD mice, and WT littermate controls were tested ($n = 8-11$). Animals tested underwent acquisition training to learn to use distal and proximal cues to navigate a direct path to a hidden platform. Escape latencies of young mice (A) decreased progressively over 5 days of training

regardless of the genotype. Furthermore, aged WT mice (B) showed a progressive improvement in the escape latency over time. The escape latencies for aged Tg4-42 and 5XFAD did not improve over the 5 days of training. Swimming speed was not affected in all mice tested. Escape latency and swimming speed: repeated measures ANOVA followed by Bonferroni multiple comparisons. m age in months.

exhibited comparable degrees of freezing (Figure 3). When mice were tested for context fear conditioning 24 h after the training trial, Tg4-42 and 5XFAD mice demonstrated no significantly increased freezing behavior in response to the conditioning chamber (Figure 3). In contrast, WT mice displayed significantly increased freezing (One-way ANOVA, $p < 0.001$) as a response to the context.

Tg4-42 and 5XFAD mice jumped and vocalized in response to the electric foot-shock to a similar degree as WT mice, suggesting normal pain perception in these mutant mice. However, transgenic mice were not able to attribute the pain of the foot-shock during the training trial to the context. Therefore, Tg4-42 and 5XFAD show impaired contextual learning.

5XFAD MICE SHOW IMPAIRED TONE LEARNING

Twenty-four hours after the context testing (48 h after training), the same mice were tested for conditioned fear of a tone. Therefore, mice were reintroduced to the altered fear conditioning chamber. When the tone was presented without the foot-shock, both Tg4-42 and WT mice exhibited similar freezing responses (Figure 4). In both mouse lines, freezing increased significantly compared to the pre-tone period (One-way ANOVA, WT, and Tg4-42: $p < 0.001$). However, 5XFAD mice demonstrated substantially less freezing behavior in response to the tone. 5XFAD mice did not associate the tone with the previously received foot-shock as freezing

was not significantly different between the training and the tone trial.

These results indicate that Tg4-42 mice exhibit a selective impairment of contextual fear learning (see previous sections), while their tone learning ability remains intact. 5XFAD mice on the other hand demonstrate both impaired contextual and tone fear learning.

DEEP SEQUENCING OF MOUSE BRAINS

In total, deep sequencing identified 15,711,910 and 16,143,760 sequence reads for young and old wildtype mice, respectively. For young wildtype mice, 6,230,197 reads (39.65%) and for old wildtype mice, 5,512,056 reads (34.14%) were mapped to exons. In young 5XFAD mice, the read mapping revealed 8,570,239 (60.28%) of 14,216,258 reads in exonic regions. Out of 18,288,161 reads, 9,163,060 (50.10%) hit exons in old 5XFAD mice. The brain exome of young Tg4-42 mice was covered by 6,342,018 (47.28%) out of 13,414,301 reads. For old Tg4-42 mice, 12,488,206 reads were detected in total, of which 4,976,552 (39.85%) could be mapped to exons. The numbers of exonic reads are summarized in Table 1.

DEEP SEQUENCING IDENTIFIED OVER-EXPRESSED TRANSGENES

5XFAD mice over-express human amyloid precursor protein (APP695) carrying the Swedish, London, and Florida mutations as

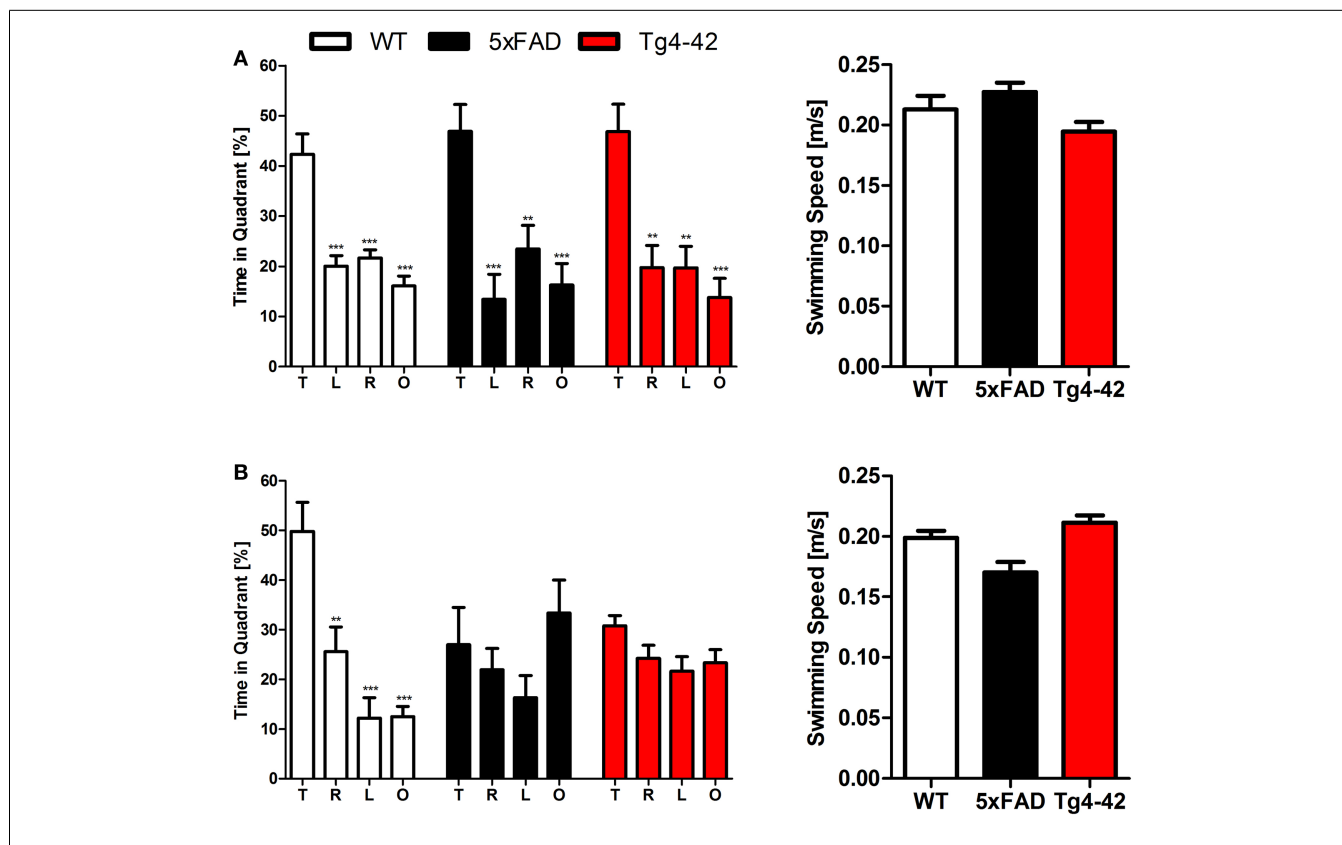


FIGURE 2 | Spatial reference memory deficits in aged Tg4-42 and 5XFAD mice shown in the probe trial of the Morris water maze. Female young and aged Tg4-42 mice, 5XFAD mice, and WT littermate controls were tested ($n = 8-11$). The probe trial was given at the end of learning phase (acquisition training) to assess spatial reference memory. Quadrant preference and swimming speed for the first 30 s of the probe trial were analyzed. **(A)** Young Tg4-42, 5XFAD, and WT mice showed no impairment in spatial reference memory. All groups spent a significant greater percentage of time in the target quadrant (WT: $p < 0.001$ T vs. all other quadrants; 5XFAD: $p < 0.001$ T

vs. L and O, $p < 0.01$ T vs. R; Tg4-42: $p < 0.001$ T vs. O, $p < 0.01$ T vs. R and L). The swimming speed did not differ between the groups. **(B)** Probe trial revealed a significant reduced learning behavior for aged Tg4-42 and 5XFAD mice as they showed no preference for the target quadrant. WT mice have no learning deficits at this age (WT: $p < 0.001$ T vs. L and O, $p < 0.01$ T vs. R). Swimming speed did not differ between the groups. T, target quadrant; L, left quadrant; R, right quadrant; O, opposite quadrant. Quadrant preference and swimming speed; One-way analysis of variance (ANOVA) followed by Bonferroni multiple comparisons. *** $p < 0.001$; ** $p < 0.01$.

well as human presenilin-1 (PSEN-1) carrying the M146L/L286V mutations. Both peptides are expressed under the control of the neuronal Thy-1 promoter (Oakley et al., 2006). As expected, sequence reads pertaining to PSEN-1, APP, and a Thy-1 promoter sequence (Moechars et al., 1996) were over-represented in both young and aged old 5XFAD brains (data not shown) and therefore served as a positive and internal control for RNA-Seq.

In Tg4-42 mice, a Thy-1 promoter sequence (Moechars et al., 1996) was found to be over-expressed in both young and aged mice (data not shown). Again, this was expected as Tg4-42 mice express human A β_{4-42} fused to the murine TRH signal peptide under the control of the neuronal Thy-1 promoter (Bouter et al., 2013).

GENE EXPRESSION IN YOUNG Tg4-42 AND 5XFAD MICE

Nineteen genes were identified as significantly differentially expressed between young 5XFAD and age-matched WT mice. In order to demonstrate the expression changes, volcano plots were created (Figure 5A). Thirteen genes were up-regulated (Figure 5A, green dots), while six genes were down-regulated (Figure 5A, red

dots). DEGs encoded proteins from diverse functional categories, including translation (ribosomal proteins), glycolysis, and ATP-binding, kinases and hydrolases (Table 2). In contrast, no DEGs could be detected in young Tg4-42 mice.

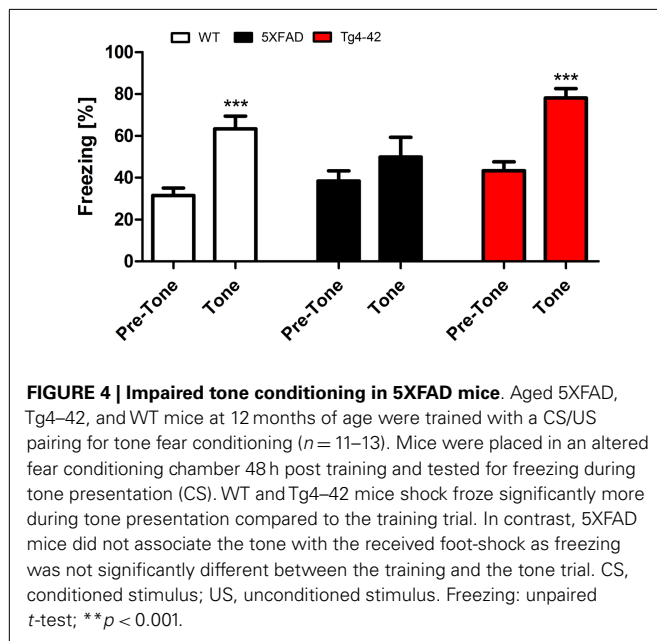
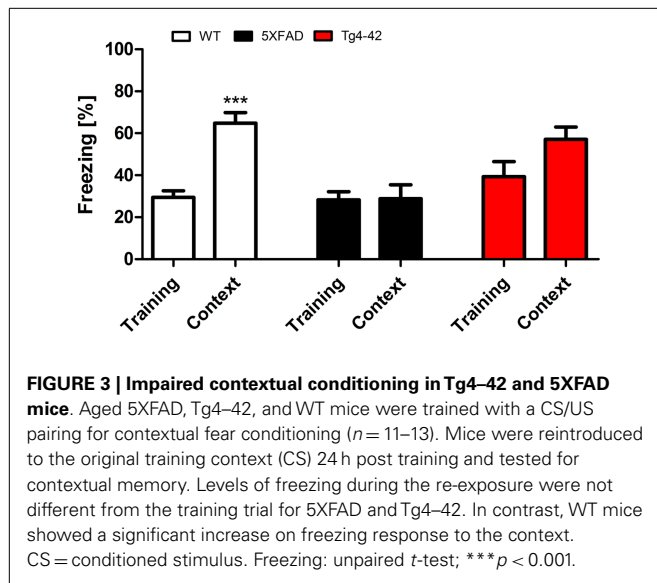
GENE EXPRESSION IN AGED Tg4-42 MICE

Fifty-six genes were differentially expressed in aged Tg4-42 mice. Seven genes were up-regulated and 49 down-regulated (Figure 5C). Twenty genes were solely differentially expressed in aged Tg4-42 (Table 3; Figure 6), among these only three genes were found to be up-regulated (*Uqc2*, *Beta-S*, and *Kif1a*).

The 17 genes that were significantly down-regulated are involved in diverse biological processes including regulation of gene expression, nervous system development, cell communication, metal ion transport, neurogenesis, and regulation of synaptic plasticity.

GENES SIMILARLY EXPRESSED IN BOTH AGED Tg4-42 AND 5XFAD MICE

Of the 56 DEGs in aged Tg4-42 mice, 36 were also found to be differentially expressed in aged 5XFAD mice (Table 4; Figure 6).



Of these 36 genes, four were up-regulated and 32 were down-regulated in aged Tg4-42 and 5XFAD mice and most showed similar expression levels in the two models.

The biggest differences between aged Tg4-42 and 5XFAD could be detected in the expression of *Gfap* and *Xist*. The intermediate filament protein GFAP encoding gene was found to be four times higher over-expressed in 5XFAD compared to Tg4-42. The non-protein coding RNA *Xist* was twofold less abundant in Tg4-42 as compared to 5XFAD mice. Apart from *Gfap*, *Calmodulin 3*, *Fbxo2*, and *Gpm6a* were also up-regulated in both aged mouse lines.

The functional annotation of the jointly down-regulated genes includes the following gene ontology (GO) (Ashburner et al., 2000) categories: regulation of cell differentiation and anatomical structure development, regulation of gene expression and transcription,

Table 1 | Number of exonic reads in brain tissue of wildtype and transgenic mice.

Genotype	Number of reads in exons
Young WT	6,230,197
Aged WT	5,512,056
Young 5XFAD	8,570,239
Aged 5XFAD	9,163,060
Young Tg4-42	6,342,018
Aged Tg4-42	4,976,552

histone modification, ion binding and protein methyltransferase activity, nervous system development, and neurogenesis.

Two genes were similarly down-regulated in aged Tg4-42 and 5XFAD but also young 5XFAD animals (Figure 6). First, *Ubqln2* which encodes a member of the ubiquilin family (Ubiquilin 2) that is involved in the protein degrading pathway as it regulates the degradation of ubiquitinated proteins (Ko et al., 2004). Second, the RNA binding protein neuro-oncological ventral antigen 2 encoding gene (*Nova2*).

GENE EXPRESSION IN AGED 5XFAD MICE

In aged 5XFAD mice, 131 genes with significant expression changes were identified. While 62 genes were up-regulated, 69 genes were down-regulated (Figure 5B). Eighty-seven of the genes were only found to be altered in aged 5XFAD mice (Table 5), while 36 showed an overlap with aged Tg4-42 mice (Table 4; Figure 6) and eight were also differentially expressed in young 5XFAD mice.

A notable group DEGs is involved in immune system processes and inflammation (according to the GO annotation). These are, among others, innate immune response and adaptive immune response, immune effector processes, activation and regulation of immune response as well as immune system development.

Furthermore, DEGs were also involved in cell communication and system development, signal transduction, synaptic transmission as well as regulation of gene expression and transcription.

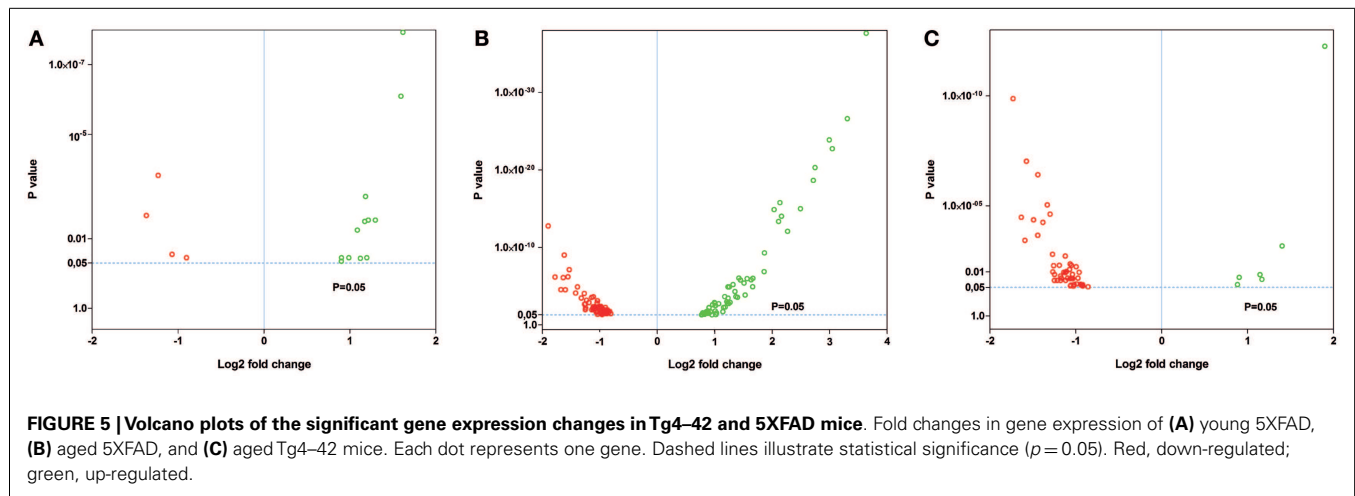
GENES SIMILARLY EXPRESSED IN BOTH YOUNG AND AGED 5XFAD MICE

Eight genes were found to be differentially expressed in both young and aged 5XFAD mice (Figure 6). Of these genes, four were up-regulated and four down-regulated. The up-regulated genes are the ribosomal protein *Rpl21*, *Aldolase A*, *Snora68*, and the ribonuclease P RNA component H1. *Ubqln2*, *Nova2*, *Atp1a2*, and *Rn45s* showed reduced expression.

VALIDATION OF DIFFERENTIALLY EXPRESSED GENES IDENTIFIED BY RNA-Seq USING REAL-TIME PCR

The quality of the isolated RNA is crucial for obtaining reliable qRT-PCR results. Therefore, the quality of the RNA samples isolated from the mice brains was evaluated by assessing the integrity and purity of the RNA. All samples displayed A260/A230 ratios greater than 1.8 and A260/A280 ratios higher than 2.0 (data not shown) indicating an acceptable RNA purity.

For young 5XFAD (Figure 7), aged 5XFAD (Figure 8), and Tg4-42 (Figure 9) mice at least seven DEGs were randomly selected



and validated using qRT-PCR. For all genes, the qRT-PCR analysis revealed expression patterns similar to the deep sequencing results.

DISCUSSION

The transcriptome includes all RNA transcripts expressed in a given tissue and renders a profile of genes that are expressed at the studied time point. Altered gene expression profiles may therefore provide information about the genes and mechanisms involved in the molecular pathogenesis of diseases like AD and ultimately promote the search for new therapeutic drugs.

ADVANTAGES OF mRNA DEEP SEQUENCING

Microarrays were used in the past as a standard technique for transcriptome profiling. The method has been proven to be valuable to quantify simultaneously large numbers of mRNA transcripts (Courtney et al., 2010). Commercially available microarrays can be used to analyze up to 15,000–30,000 different mRNAs and facilitate genome-wide gene expression profiling (Altar et al., 2009). Oligonucleotide and cDNA microarrays are both affordable and offer a high-throughput approach.

However, due to the use of indirect signal detection by hybridization, microarray techniques possess several limitations (Courtney et al., 2010). These include reliance upon knowledge of already known sequences, poor range of quantification, and relatively low sensitivity and specificity (Choi et al., 2013). Furthermore, the non-specific binding of samples make the detection of low expressed transcripts against the background noise difficult (Sutherland et al., 2011) and unsuitable for the quantification of over- and under-expressed genes with fold changes smaller than two (Wang et al., 2009). van Bakel et al. (2010) reported that hybridization signals from microarrays can lead to a high number of false positive signals especially from transcripts with low expression levels.

Several microarray studies on amyloid mouse models for AD have been reported (Stein and Johnson, 2002; Dickey et al., 2003; Wu et al., 2006; Selwood et al., 2009; Wirz et al., 2013). The transgenic models included APP/PS1 Δ Ex9, PDAPP, Tg2576, and combinations with different mutant PSEN-1 genetic variants. All of these transgenic lines represent models for familial AD and

abundant plaque formation without severe neuron loss. Therefore, we compared two models that do show a robust behavioral deficit and in addition harbor a significant neuron loss.

RNA-Seq allows to cope with many of the problems described for microarrays and has a number of advantages over microarray technology. Most importantly, deep sequencing does not rely on known genome sequence data and therefore novel transcripts can be detected (Courtney et al., 2010). It is possible to detect billions of nucleotide information within a single experiment (Cheng et al., 2013). Furthermore, problems with saturation and background signal do not exist as each molecule is individually sequenced and mapped to unique regions of the genome. RNA-Seq offers a larger dynamic range than microarray technology as no upper or lower levels exist in this quantification technique (Courtney et al., 2010). In comparison to microarrays, deep sequencing has a low false positive rate and is moreover highly reproducible (Nagalakshmi et al., 2008).

5XFAD, A MODEL FOR FAMILIAL ALZHEIMER'S DISEASE

Using deep sequencing technology, we analyzed the RNA profiles from the two AD models 5XFAD and Tg4–42 (Table 6). We compared these two models, because they show a robust behavioral deficit and in addition develop a significant neuron loss.

5XFAD is a model for familial AD that shows massive and early plaque formation, intraneuronal A β aggregation, behavioral deficits, and neuron loss in the neocortical layer 5 and subiculum (Oakley et al., 2006; Jawhar et al., 2010). In the 5XFAD model, many molecular pathways are altered due to mutant APP and PS1 over-expression leading to massive elevation of A β _{1–42}, A β _{1–40}, A β _{4–42}, pyroglutamate A β _{pE3–42}, and A β _{3–42} (Wittnam et al., 2012). The consequence of this is that 5XFAD harbor soluble forms of full-length and diverse N-truncated A β species that are also found precipitated in plaques.

Tg4–42, A MODEL FOR SPORADIC ALZHEIMER'S DISEASE

In vitro and *in vivo* analysis of amyloid deposits in AD revealed N- and C-terminal variants of the A β peptide (Masters et al., 1985; Prelli et al., 1988; Miller et al., 1993). Masters et al. (1985) discovered that the majority (64%) of the peptides in amyloid

Table 2 | List of differentially expressed transcripts in young 5XFAD mice.

ID	Gene name	Gene description	GO biological process annotation/functions	Log2 fold change	Adjusted p-value
MGI:87994	<i>Aldoa</i>	Aldolase A, fructose-bisphosphate	Fructose-bisphosphate aldolase activity Actin binding Cytoskeletal protein binding Tubulin binding Glycolysis	1.62	1.16E-08
MGI:2148181	<i>Snora68</i>	Small nucleolar RNA, H/ACA box 68	Non-coding RNA Uridine modifications	1.60	7.99E-07
MGI:105110	<i>Rps2</i>	Ribosomal protein S2	mRNA binding Fibroblast growth factor binding Structural constituent of ribosome	1.30	2.92E-03
MGI:96412	<i>Ide</i>	Insulin-degrading enzyme	Insulysin activity Metalloendopeptidase activity Protein homodimerization activity Hydrolase Activity Beta-amyloid binding Glycoprotein binding ATP-binding Zinc ion binding Ubiquitin binding	1.22	2.92E-03
MGI:1353472	<i>Rpl7a</i>	Ribosomal protein L7a	RNA binding Structural constituent of ribosome	1.20	3.51E-02
MGI:98865	<i>Ttr</i>	Transthyretin	Hormone activity Protein heterodimerization activity Retinol binding	1.18	6.09E-04
MGI:1340062	<i>Sgk1</i>	Serum/glucocorticoid regulated kinase 1	Kinase activity Potassium/calcium channel regulator activity ATP-binding Response to DNA damage stimulus	1.17	3.16E-03
MGI:1278340	<i>Rpl21</i>	Ribosomal protein L21	Structural constituent of ribosome RNA binding	1.12	3.65E-02
MGI:108415	<i>Pafah1b2</i>	Platelet-activating factor acetylhydrolase, isoform 1b, subunit 2	Hydrolase activity 1-Alkyl-2 acetyl-glycero-phosphocholine esterase activity Homodimerization activity	1.09	5.67E-03
MGI:99845	<i>Gdi2</i>	Guanosine diphosphate (GDP) dissociation inhibitor 2	Rab GDP-dissociation inhibitor activity Rab GTPase activator activity	0.99	3.51E-02
MGI:1934664	<i>Rpph1</i>	Ribonuclease P RNA component H1	Endoribonuclease activity	0.90	3.51E-02
MGI:97783	<i>Psap</i>	Prosaposin	Glycoprotein Lipid binding Enzyme activator activity	0.90	3.51E-02
MGI:97591	<i>Pkm</i>	Pyruvate kinase, muscle	Magnesium ion binding ATP-binding Potassium ion binding Pyruvate kinase activity	0.90	4.41E-02

(Continued)

Table 2 | Continued

ID	Gene name	Gene description	GO biological process annotation/functions	Log2 fold change	Adjusted p-value
MGI:108391	<i>Kif1a</i>	Kinesin family member 1A	ATP-binding Phospholipid binding Motor activity Axonal neuropathies	−0.90	3.51E-02
MGI:88106	<i>Atp1a2</i>	ATPase, Na ⁺ /K ⁺ transporting, alpha 2 polypeptide	Sodium:potassium-exchanging ATPase activity ATP-binding Metal ion binding Hydrolase activity	−0.90	3.51E-02
MGI:1860283	<i>Ubqln2</i>	Ubiquilin 2	Protein binding Cell death	−1.07	2.82E-02
MGI:1313261	<i>Spnb3</i>	Spectrin beta, non-erythrocytic 2	Phospholipid binding Actin binding Structural constituent of cytoskeleton	−1.23	1.50E-04
MGI:1337000	<i>Rn45s</i>	45S pre-ribosomal 5	Non-coding RNA	−1.23	1.50E-04
MGI:104296	<i>Nova2</i>	Neuro-oncological ventral antigen 2	RNA binding	−1.37	2.14E-03

plaques of AD begin with a phenylalanine residue corresponding to position 4 of the full-length sequence. Moreover, they detected dimeric and tetrameric A β aggregates from the HPLC separations of plaques from AD having the same ragged NH₂-terminal ends. The importance of A β _{4–42} was later supported by the finding that it represents a dominant fraction in the hippocampus and cortex of AD patients using immunoprecipitation and mass spectrometry (Portelius et al., 2010).

In order to investigate the long-lasting neurotoxic effect of A β _{4–42}, we recently generated the novel mouse model Tg4–42 expressing exclusively A β _{4–42} (Bouter et al., 2013). Tg4–42 mice develop severe hippocampal neuron loss and memory deficits that correlate well with the hippocampus-specific intraneuronal expression of A β _{4–42}. These findings are corroborated by previous mouse models expressing full-length mutant APP. For example, APP/PS1KI mice exhibit neuron loss in the CA1 region of the hippocampus (Casas et al., 2004; Breyhan et al., 2009), the frontal cortex (Christensen et al., 2008), and in distinct cholinergic nuclei (Christensen et al., 2010). The APP/PS1KI model is characterized by age-dependent accumulation of heterogeneous N-terminal truncated A β peptides with A β _{4–42} being one of the most abundant variants (Casas et al., 2004). In 5XFAD mice, a heterogeneous mixture of full-length, N-truncated and modified A β peptides, including A β _{4–42}, was also found (Wittnam et al., 2012). Hence, the pathological events observed in the APP/PS1 KI and 5XFAD mouse models might be at least partly triggered by N-terminal truncated A β _{4–42}.

LEARNING AND MEMORY DEFICITS IN 5XFAD AND Tg4–42 MICE

In the present work, we could show that Tg4–42 mice and 5XFAD mice feature comparable learning and memory deficits. Both mouse lines exhibited age-dependent spatial reference memory

deficits as assessed by the Morris water maze. Aged Tg4–42 and 5XFAD mice have also been tested in the CFC paradigm and exhibited deficits in this hippocampus-dependent memory tasks. Tg4–42 and 5XFAD mice displayed hippocampus-dependent memory deficits similar to those of other AD transgenic models (Chen et al., 2000; Stover and Brown, 2012; Kishimoto et al., 2013).

Classical fear conditioning is assumed to be highly dependent on the hippocampus (Bast et al., 2003). Phillips and LeDoux (1992) reported that lesions of the hippocampus interfered with CFC but not with cue and TFC. In contrast, a functional amygdala is required for appropriate fear conditioning for both context and tone. Moreover, anxiety behavior was claimed to correlate with the presence of intraneuronal A β in the amygdala (España et al., 2010). These observations are in agreement with the impairment in conditioned learning in response to a tone stimulus of aged 5XFAD mice, but not of age-matched Tg4–42 animals.

DEEP SEQUENCING IN 5XFAD AND Tg4–42 MICE

In order to detect gene expression changes in the two AD mouse models, deep sequencing analysis was performed on young as well as aged 5XFAD and Tg4–42 mice. A wide range of DEGs could be identified in aged Tg4–42 as well as in young and aged 5XFAD mice compared to age-matched wildtype controls, respectively. Even though, the potential for false positive results cannot be eliminated completely, more than 25 transcript changes detected by RNA-Seq could be successfully validated by qRT-PCR and therefore validated the deep sequencing results. Furthermore, the detection of the transgenic human PSEN-1 and APP sequences in young and aged 5XFAD mice through deep sequencing is also an indication for the quality of the method.

The expression changes detected in the transgenic mice give a broad picture of the profound physiological changes that

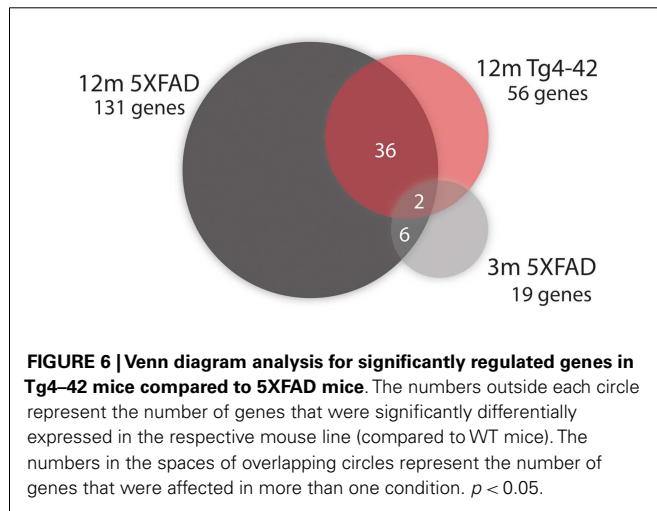
Table 3 | List of transcripts exclusively differentially expressed in aged Tg4-42.

ID	Gene name	Gene description	GO biological process annotation/functions	log2 Fold change	Adjusted p-value
MGI:1914517	<i>Uqcc2</i>	Ubiquinol-cytochrome-c reductase complex assembly factor 2	Regulation of insulin secretion ATP production	1.17	2.18E-02
MGI:5474852	<i>Beta-S</i>	Hemoglobin, beta adult s chain	Iron ion binding Oxygen binding	1.14	1.31E-02
MGI:108391	<i>Kif1a</i>	Kinesin family member 1A	Microtubule motor activity ATP-binding	0.90	1.77E-02
MGI:2153272	<i>Ttrap</i>	Transformation/transcription domain-associated protein	Phosphotransferase Activity Regulation of transcription	-0.86	4.74E-02
MGI:1194504	<i>Kcnj10</i>	ATP-sensitive inward rectifier potassium channel 10	Potassium channel activity ATP-binding	-0.93	3.76E-02
MGI:3039582	<i>Lmtk3</i>	Lemur tyrosine kinase 3	Protein tyrosine kinase activity	-0.94	3.98E-02
MGI:1343180	<i>Vgf</i>	Nerve growth factor inducible	Neuropeptide hormone activity Synaptic plasticity Neurosecretory protein (Jahn et al., 2011 no. 284) Regulation of energy balance (Jahn et al., 2011 no. 284) Important for modulating neuronal activity (Cocco et al., 2010 no. 286)	-0.95	3.64E-02
MGI:106374	<i>Zmiz2</i>	Zinc finger MIZ domain containing protein 2	Zinc ion binding Ligand-dependent nuclear receptor transcription coactivator activity	-0.98	1.90E-02
MGI:1194488	<i>Slc32a1</i>	Vesicular inhibitory amino acid transporter solute carrier family 32 (GABA vesicular transporter), member 1	Glycine transporter activity Amino acid-polyamine transporter activity Neurotransmitter transport	-1.02	3.76E-02
MGI:1277171	<i>Dcx</i>	Doublecortin	Microtubule binding Protein kinase binding Neurogenesis	-1.03	4.42E-02
MGI:101947	<i>Hnrnpd</i>	Heterogeneous nuclear ribonucleoprotein D	Regulation of transcription RNA binding and telomeric DNA binding	-1.04	1.99E-02
MGI:109591	<i>Nfic</i>	Nuclear factor I/C	Transcription factor activity DNA binding	-1.10	1.90E-02
MGI:2441726	<i>BC005537</i>	cDNA sequence BC005537	Unknown	-1.11	9.46E-03
MGI:2673998	<i>Arhgap33</i>	Rho GTPase activating protein 33	Rac GTPase activator activity Phosphatidylinositol binding	-1.12	1.08E-02
MGI:1330828	<i>Cdk5r2</i>	Cyclin-dependent kinase 5 activator 2 (p39)	Lipid binding Cyclin-dependent protein kinase 5 Activator activity Neuron-specific	-1.14	1.04E-02
MGI:2674092	<i>Zfp609</i>	Zinc finger protein 609	Zinc ion binding	-1.17	1.90E-02
MGI:1915454	<i>2900060</i> <i>B14Rik</i>	RIKEN cDNA 2900060B14 gene	Unknown	-1.18	2.43E-02

(Continued)

Table 3 | Continued

ID	Gene name	Gene description	GO biological process annotation/functions	log2 Fold change	Adjusted p-value
MGI:1351334	<i>Syn3</i>	Synapsin III	Catalytic activity ATP-binding	-1.25	1.30E-02
MGI:1920907	<i>Fbrs1</i>	Fibrosin-like 1	Unknown	-1.25	2.43E-02
MGI:106589	<i>Hivep3</i>	Human immunodeficiency virus type I enhancer binding protein 3	DNA binding Zinc ion binding Transcription factor	-1.26	5.18E-03



COMMON MOLECULAR SIGNATURE OF Tg4-42 AND 5XFAD MICE

Interestingly, 36 genes were differentially expressed in both mouse models indicating common disease pathways associated with behavioral deficits and neuron loss occurring in these mouse models. Nearly half of the DEGs in aged Tg4-42 were also differentially expressed in 5XFAD mice.

Many of the genes that showed differential regulation in 5XFAD alone belong to neuroinflammatory processes typically found associated with plaques. As Tg4-42 mice do not develop any plaques, but massive neuron loss, we assume that the genes isolated in both models and those in Tg4-42 alone are defining the molecular signature underlying memory decline in this mouse model for AD.

The DEGs that were found in both models fall in a broad range of functional categories: regulation of cell differentiation and anatomical structure development, regulation of gene expression and transcription, histone modification, ion binding and protein methyltransferase activity, nervous system development, and neurogenesis.

Together with *Calm3*, *Fbxo2*, and *Gpm6a* only *Gfap* was found to be up-regulated in both aged 5XFAD and Tg4-42 mice. The astrocyte marker glial fibrillary acidic protein gene (*Gfap*) was found to be similarly up-regulated in both mouse lines. Increased astrogliosis was previously described in both mouse lines (Oakley et al., 2006; Bouter et al., 2013). Increased astrogliosis, measured by GFAP concentration, is also found in cortex, thalamus, brainstem, and cerebellum in AD brains (Delacourte, 1990).

Next to the up-regulated genes, 32 genes were commonly down-regulated in aged transgenic mice compared to WT. Among others *Lrp1* was altered. Kanekiyo et al. (2013) demonstrated that receptor-mediated endocytosis in neurons by LRP1 plays a critical role in A β clearance in the brain.

Decreased levels of *Shank1* RNA were found in both mouse lines. The levels of the post-synaptic proteins SHANK1 and SHANK3 were also regulated in patients with AD and in the brains of amyloid precursor protein transgenic mice. It has been proposed that A β reduces Shank levels in the dendrites (Pham et al., 2010).

The gene coding for the lysine (K)-specific methyltransferase 2D (*Mll2*), also known as *Kmt2b*, that is highly expressed throughout development as well as in adult tissue (Glaser et al., 2006) is down-regulated in aged 5XFAD and Tg4-42. Kerimoglu et al. (2013) showed that mice lacking *Mll2* in the adult forebrain

accompany the neuron loss and the detected memory deficits in 5XFAD and Tg4-42 mice. Some of the DEGs have been reported before, while many genes are described for the first time in the context of AD. The observed parallel expression of these genes now offers new perspectives in understanding the pathology of AD.

DIFFERENTIALLY EXPRESSED GENES IN YOUNG 5XFAD MICE

In young 5XFAD mice, a substantial number of genes is differentially expressed prior to robust amyloid deposition and neuron loss. The 19 DEGs encoded proteins from diverse functional categories, including translation, glycolysis, and ATP-binding, kinases and hydrolases. The 5XFAD model has been reported to develop plaque deposition starting already at the age of 3 months (Jawhar et al., 2010). Intraneuronal A β is evident at 1.5 months of age, just before the first appearance of amyloid deposits at 2 months of age (Oakley et al., 2006).

The data of young 5XFAD mice elucidate the expression profile at the commencement of plaque formation and before learning and memory deficits are apparent. Several DEGs that are involved in the clearance of A β : transthyretin (*Tr*) (Li and Buxbaum, 2011) and insulin-degrading enzyme (*Ide*) (Farris et al., 2003; Miners et al., 2009) are found up-regulated.

No DEGs were detected in young Tg4-42 mice, which suggest that the pathology is weak at that age and points to a later onset of the pathological events that underlie the phenotypic changes observed at later ages.

Table 4 | List of transcripts differentially expressed in both aged Tg4-42 and 5XFAD mice.

ID	Gene name	Gene description	GO biological process annotation/functions	log2 Fold change Tg4-42	Adjusted p-value Tg4-42	log2 Fold change 5xFAD	Adjusted p-value 5xFAD
MGI:103249	<i>Calm3</i>	Calmodulin 3	Ion channel binding Calcium ion binding G-protein coupled receptor protein signaling pathway	1.90	5.49E-13	1.00	1.28E-03
MGI:2446216	<i>Fbxo2</i>	F-box protein 2	Ubiquitin-protein ligase activity Glycoprotein binding Beta-amyloid binding Carbohydrate binding	1.40	6.60E-04	1.24	1.73E-03
MGI:107671	<i>Gpm6a</i>	Neuronal membrane glycoprotein M6-a	Calcium channel activity involved in neuronal differentiation Role in neuronal plasticity	0.90	1.77E-02	0.90	5.39E-03
MGI:95697	<i>Gfap</i>	Glial fibrillary acidic protein	Integrin binding Kinase binding Structural constituent of cytoskeleton	0.88	3.76E-02	3.64	2.36E-42
MGI:1860283	<i>Ubqln2</i>	Ubiquilin 2	Ubiquitin binding Protein modification Proteolysis	-0.92	4.35E-02	-1.27	8.71E-05
MGI:97495	<i>Pbx1</i>	Pre-B-cell leukemia transcription factor 1/pre-B-cell leukemia homeobox 1	Transcription factor activity Protein heterodimerization activity involved in the regulation of osteogenesis required for skeletal patterning and programing	-0.92	3.79E-02	-0.86	2.85E-02
MGI:3647820	<i>Gm15800</i>	Predicted gene 15800	Ubiquitin-protein ligase activity	-0.96	1.04E-02	-0.83	1.84E-02
MGI:96669	<i>Kcnc3</i>	Potassium voltage-gated channel, shaw-related sub-family, member 3	Voltage-gated potassium channel activity Delayed rectifier potassium channel activity	-0.99	3.47E-02	-1.04	6.53E-03
MGI:96828	<i>Lrp1</i>	Low density lipoprotein receptor-related protein 1	Endocytic receptor or receptor activity Lipoprotein binding Calcium ion binding Apolipoprotein binding Beta-amyloid clearance Apoptotic cell clearance	-1.00	5.80E-03	-0.83	1.77E-02
MGI:2183691	<i>Nav2</i>	Neuron navigator 2	Heparin binding Helicase activity ATP-binding Role in neuronal development	-1.04	1.29E-02	-0.89	2.33E-02
MGI:1890563	<i>Wasf1</i>	WAS protein family, member 1	Actin binding	-1.05	1.99E-02	-0.95	2.11E-02
MGI:96995	<i>Mll1</i>	Lysine (K)-specific methyltransferase 2A	Calcium ion binding Zinc ion binding Chromatin binding Histone methyltransferase activity Regulation of transcription	-1.05	4.97E-03	-0.81	3.37E-02

(Continued)

Table 4 | Continued

ID	Gene name	Gene description	GO biological process annotation/functions	log2 Fold change Tg4-42	Adjusted p-value Tg4-42	log2 Fold change 5xFAD	Adjusted p-value 5xFAD
MGI:2446229	<i>Tet3</i>	Tet methylcytosine dioxygenase 3	Methylcytosine dioxygenase activity Oxidoreductase activity Metal ion binding Plays role in the DNA methylation process	-1.05	1.98E-02	-1.05	6.56E-03
MGI:99948	<i>Zfx3</i>	Zinc finger homeobox 3	GTP binding Sequence-specific DNA binding transcription factor activity Zinc ion binding	-1.06	3.98E-02	-1.12	7.24E-03
MGI:1347464	<i>Foxg1</i>	Forkhead box G1	Sequence-specific DNA binding Negative regulation of neuron differentiation Regulation of transcription Brain development Forebrain marker (Yahata et al., 2011 no. 296)	-1.06	4.30E-02	-1.11	9.22E-03
MGI:1919847	<i>Auts2</i>	Autism susceptibility candidate 2	Unknown	-1.07	2.00E-02	-1.05	7.45E-03
MGI:1915467	<i>Prrc2a</i>	Proline-rich coiled-coil 2A	Unknown	-1.07	4.33E-03	-0.85	2.24E-02
MGI:1917685	<i>Inf2</i>	Inverted formin, FH2 and WH2 domain containing	Rho GTPase binding actin binding	-1.07	7.70E-03	-0.87	2.60E-02
MGI:2158663	<i>Inpp5j</i>	Inositol polyphosphate 5-phosphatase J	SH3 domain binding Hydrolase activity Phosphatase activity	-1.12	2.43E-02	-1.78	6.55E-07
MGI:2682319	<i>Mll2</i>	Lysine (K)-specific methyltransferase 2D	Histone methyltransferase	-1.12	1.90E-03	-1.05	1.48E-03
MGI:3026647	<i>Flrt1</i>	Fibronectin leucine rich transmembrane protein 1	Receptor signaling protein activity	-1.18	1.53E-02	-1.25	1.89E-03
MGI:1888520	<i>Brd4</i>	Bromodomain containing 4	DNA binding	-1.19	4.97E-03	-1.05	7.64E-03
MGI:1916205	<i>Srrm4</i>	Serine/arginine repetitive matrix 4	mRNA binding Promotes alternative splicing and inclusion of neural-specific exons in target mRNAs	-1.22	2.43E-02	-1.25	6.20E-03
MGI:1926106	<i>Fam163b</i>	Family with sequence similarity 163, member B	Unknown	-1.27	9.85E-03	-1.60	2.91E-05
MGI:2685951	<i>Myo16</i>	Myosin XVI	Motor activity ATP-binding Protein phosphatase binding	-1.27	1.57E-03	-1.09	4.62E-03
MGI:1923304	<i>Prrc2b</i>	Proline-rich coiled-coil 2B	Unknown	-1.30	2.37E-05	-1.11	2.28E-04
MGI:1923206	<i>Srrm2</i>	Serine/arginine repetitive matrix 2	C ₂ H ₂ zinc finger domain binding RNA binding involved in pre-mRNA splicing	-1.33	8.92E-06	-1.04	7.25E-04

(Continued)

Table 4 | Continued

ID	Gene name	Gene description	GO biological process annotation/functions	log2 Fold change Tg4-42	Adjusted p-value Tg4-42	log2 Fold change 5xFAD	Adjusted p-value 5xFAD
MGI:1337080	<i>Ncor2</i>	Nuclear receptor co-repressor 2	Chromatin binding Regulation of transcription Transcription co-repressor activity Notch binding	-1.38	5.62E-05	-1.39	1.21E-05
MGI:1306776	<i>Mtap1a</i>	Microtubule-associated protein 1 A	Structural molecule activity Microtubule assembly Perception of sound	-1.44	3.82E-07	-1.62	9.68E-10
MGI:104725	<i>Atn1</i>	Atrophin 1	Toxin receptor binding Transcription co-repressor activity	-1.44	2.15E-04	-1.32	3.38E-04
MGI:104296	<i>Nova2</i>	Neuro-oncological ventral antigen 2	RNA binding	-1.49	4.27E-05	-1.64	7.71E-07
MGI:3613677	<i>Shank1</i>	SH3 and multiple ankyrin repeat domains 1	SH3 domain binding Identical protein binding Synapse maturation	-1.57	9.26E-08	-1.53	7.43E-08
MGI:2679002	<i>Prr12</i>	Proline-rich 12	DNA binding	-1.59	3.68E-04	-1.68	2.80E-05
MGI:2143886	<i>Dot1l</i>	DOT1-like histone H3 methyltransferase	Transcription factor binding DNA binding Histone-lysine N-methyltransferase activity	-1.63	3.29E-05	-1.06	1.72E-02
MGI:88107	<i>Atp1a3</i>	Sodium/potassium-transporting ATPase subunit alpha-3	Sodium:potassium-exchanging ATPase activity ATP-binding Metal ion binding Hydrolase activity	-1.73	1.31E-10	-1.90	1.70E-13
MGI:98974	<i>Xist</i>	Inactive x specific transcripts	Non-protein coding	-1.73	1.31E-10	-0.90	5.70E-03

displayed impaired hippocampus-dependent memory function. Furthermore, the loss of MLL2 leads to down-regulation of genes implicated in neuronal plasticity. 5XFAD and Tg4-42 also showed hippocampus-dependent memory impairments. The down-regulation of *Mll2* that is reported to be crucial for memory consolidation and regulation of hippocampal plasticity genes is well in line with our findings.

DIFFERENTIALLY EXPRESSED GENES IN AGED Tg4-42 MICE

Up-regulated genes in aged Tg4-42 mice

Twenty genes were solely differentially expressed in aged Tg4-42. Among these, only the genes *Uqcc2*, *Beta-S*, and *Kif1a* were found to be up-regulated. *Kif1a* is a member of the kinesin family (KIFs) (Takemura et al., 1996) and has previously been connected to AD (Kondo et al., 2012). These microtubule-based motor proteins transport membrane organelles, mRNA, and proteins (Hirokawa et al., 2009). By transporting those complexes, KIFs play important roles in neuronal function and plasticity as well as morphogenesis and survival (Hirokawa et al., 2010). In neurons, KIF1A transports components of synaptic vesicles containing synaptic vesicle proteins such as synaptophysin and synaptotagmin

(Hirokawa et al., 2010). Recently, Kondo et al. (2012) could show that an up-regulation of KIF1A contributes to synaptogenesis in the hippocampus.

Down-regulated genes in aged Tg4-42 mice

The 17 genes that were significantly down-regulated in aged Tg4-42 are involved in diverse biological processes. These include regulation of gene expression, nervous system development, cell communication, metal ion transport, neurogenesis, and regulation of synaptic plasticity. The gene encoding nerve growth factor inducible protein (VGF), which is down-regulated in aged Tg4-42, is a neurosecretory protein that is solely expressed in neurons (van den Pol et al., 1994). Adult VGF is detected in several areas in the brain including the olfactory system, cerebral cortex, hypothalamus, and hippocampus as well as the adrenal medulla and motor neurons of the spinal cord (van den Pol et al., 1994; Snyder and Salton, 1998; Thakker-Varia and Alder, 2009). Several groups proposed VGF as a potential biomarker for AD (Carrette et al., 2003; Jahn et al., 2011). They detected lower protein levels of VGF in the cerebrospinal fluid (CSF) of AD patients compared to healthy controls.

Table 5 | List of differentially expressed transcripts in aged 5XFAD mice.

ID	Gene name	Gene description	GO biological process annotation/functions	log2 Fold change	Adjusted p-value
MGI:88228	<i>C4b</i>	Complement component 4B	Endopeptidase inhibitor activity Inflammatory response Complement activation Immune response	3.31	2.44E-27
MGI:88225	<i>C1qc</i>	Complement component 1, q subcomponent, C chain	Complement activation Immune response	3.05	1.84E-23
MGI:88223	<i>C1qa</i>	Complement component 1, q subcomponent, alpha polypeptide	Phosphate transport Complement activation Immune response	2.99	1.31E-24
MGI:107341	<i>Ctss</i>	Cathepsin S	Cysteine-type peptidase activity Hydrolase activity Proteolysis Immune response	2.75	5.00E-21
MGI:88224	<i>C1qb</i>	Complement component 1, q subcomponent, beta polypeptide	Phosphate transport Complement activation Immune response	2.72	2.22E-19
MGI:1891190	<i>Ctsz</i>	Cathepsin Z	Cysteine-type peptidase activity Hydrolase activity	2.49	1.01E-15
MGI:98932	<i>Vim</i>	Vimentin	Structural constituent of cytoskeleton Identical protein binding Apoptotic process	2.27	8.36E-13
MGI:96074	<i>Hexb</i>	Hexosaminidase B	Cation binding Protein homodimerization activity Beta-N-acetylhexosaminidase activity Protein heterodimerization activity	2.16	9.49E-15
MGI:88562	<i>Ctsd</i>	Cathepsin D	Aspartic-type endopeptidase activity Hydrolase activity	2.13	1.66E-16
MGI:2148181	<i>Snora68</i>	Small nucleolar RNA, H/ACA box 68	Non-coding RNA Uridine modifications	2.11	4.37E-14
MGI:87994	<i>Aldoa</i>	Aldolase A, fructose-bisphosphate	Actin binding Fructose-bisphosphate aldolase activity Cytoskeletal protein binding Tubulin binding Glycolysis	2.03	1.32E-15
MGI:88127	<i>B2m</i>	Beta-2 microglobulin	MHC class I receptor activity Cellular defense response Innate immune response	1.86	5.03E-10
MGI:108046	<i>Laptm5</i>	Lysosomal-associated protein transmembrane 5	Transmembrane transport	1.86	1.32E-07
MGI:1333815	<i>Cx3cr1</i>	Chemokine (C-X3-C motif) receptor 1	Chemokine receptor activity G-protein coupled receptor activity Transmembrane protein Signal transduction	1.66	9.43E-07

(Continued)

Table 5 | Continued

ID	Gene name	Gene description	GO biological process annotation/functions	log2 Fold change	Adjusted p-value
MGI:99554	<i>Lgals3bp</i>	Lectin, galactoside-binding, soluble, 3 binding protein	Scavenger receptor activity Isomerase activity Cellular defense response Signal transduction	1.66	1.19E-05
MGI:1921298	<i>4632428N05Rik</i>	RIKEN cDNA 4632428N05 gene	Receptor activity	1.63	1.48E-06
MGI:96614	<i>Itgb5</i>	Integrin beta 5	Integrin binding Receptor activity Cell adhesion	1.56	1.05E-06
MGI:1914877	<i>Olfml3</i>	Olfactomedin-like 3	Scaffold protein	1.53	1.36E-04
MGI:96073	<i>Hexa</i>	Hexosaminidase A	Beta-N-acetylhexosaminidase activity Protein heterodimerization activity Hydrolase activity	1.51	3.85E-06
MGI:1339758	<i>Csf1r</i>	Colony -stimulating factor 1 receptor	Macrophage colony-stimulating factor Receptor activity Protein homodimerization activity ATP-binding Immune response	1.45	1.58E-06
MGI:107387	<i>Aqp4</i>	Aquaporin 4	Porin activity Water transmembrane transporter activity	1.42	8.90E-07
MGI:1918089	<i>P2ry12</i>	Purinergic receptor P2Y, G-protein coupled 12	ADP receptor activity Guanyl-nucleotide exchange factor activity G-protein coupled adenosine receptor activity Signal transducer activity	1.40	2.68E-04
MGI:1278340	<i>Rpl21</i>	Ribosomal protein L21	Structural constituent of ribosome RNA binding	1.37	2.20E-04
MGI:107286	<i>Man2b1</i>	Mannosidase 2, alpha B1	Carbohydrate binding Alpha-mannosidase activity Hydrolase activity	1.35	4.77E-05
MGI:1096881	<i>Eef1a1</i>	Eukaryotic translation elongation factor 1 alpha 1	GTPase activity Translation elongation factor activity Regulation of transcription	1.32	6.22E-06
MGI:1915213	<i>Npc2</i>	Niemann Pick type C2	Cholesterol binding Enzyme binding	1.27	1.20E-03
MGI:88561	<i>Ctsb</i>	Cathepsin B	Cysteine-type peptidase activity Hydrolase activity Immune response	1.25	1.21E-05
MGI:88564	<i>Ctsl</i>	Cathepsin L	Cysteine-type peptidase activity Hydrolase activity Histone binding Immune response	1.23	3.42E-04
MGI:1934664	<i>Rpph1</i>	Ribonuclease P RNA component H1	Endoribonuclease activity	1.23	1.21E-05
MGI:1920174	<i>Anln</i>	Anillin	Actin binding Phospholipid binding	1.22	1.53E-03

(Continued)

Table 5 | Continued

ID	Gene name	Gene description	GO biological process annotation/functions	log2 Fold change	Adjusted p-value
MGI:95832	<i>Grn</i>	Granulin	Growth factor activity Cytokine activity Signal transduction	1.21	1.00E-03
MGI:98729	<i>Tgfr2</i>	Transforming growth factor, beta receptor II	ATP-binding Transmembrane receptor protein serine/threonine kinase activity Transferase activity Receptor activity SMAD binding Signal transduction	1.18	4.94E-03
MGI:894320	<i>Prdx6</i>	Peroxiredoxin 6	Glutathione peroxidase activity Oxidoreductase activity Antioxidant activity Response to oxidative stress	1.17	2.21E-04
MGI:1921305	<i>Plce1</i>	Phospholipase C, epsilon 1	Guanyl-nucleotide exchange factor activity Calcium ion binding Receptor signaling protein activity Hydrolase activity Signal transducer activity	1.15	5.42E-03
MGI:107357	<i>Inpp5d</i>	Inositol polyphosphate-5-phosphatase D	SH3 domain binding PTB domain binding Hydrolase activity Signal transducer activity Immune response	1.14	1.96E-02
MGI:1330838	<i>Lgmn</i>	Legumain	Cysteine-type endopeptidase activity Peptidase activity Immune response Hydrolase activity	1.07	1.82E-03
MGI:1917329	<i>Golm1</i>	Golgi membrane protein 1	Protein modification Nucleus organization	1.03	2.85E-02
MGI:88385	<i>Cfh</i>	Complement component factor h	Heparin binding Heparan sulfate proteoglycan binding Complement activation Immune response	1.02	4.65E-02
MGI:95640	<i>Gapdh</i>	Glyceraldehyde-3-phosphate dehydrogenase	Microtubule binding NADP binding	1.01	3.07E-03
MGI:1924096	<i>Rps9</i>	Ribosomal protein S9	Structural constituent of ribosome RNA binding Translation regulator activity	1.01	1.59E-02
MGI:97171	<i>Mt1</i>	Metallothionein 1	Organic cyclic compound binding Hormone binding Copper ion binding	1.01	3.08E-03
MGI:97591	<i>Pkm</i>	Pyruvate kinase, muscle	Magnesium ion binding Pyruvate kinase activity ATP-binding	1.00	1.56E-03

(Continued)

Table 5 | Continued

ID	Gene name	Gene description	GO biological process annotation/functions	log2 Fold change	Adjusted p-value
MGI:88423	<i>Clu</i>	Clusterin	ATPase activity Ubiquitin -protein ligase binding Misfolded protein binding Immune response	0.96	2.50E-03
MGI:1338892	<i>Padi2</i>	Peptidyl arginine deiminase, type II	Protein-arginine deiminase activity Calcium ion binding Hydrolase activity Immune response	0.95	4.86E-02
MGI:1915472	<i>Tubb4b</i>	Tubulin, beta 4B class IVB	Structural molecule activity GTPase activity Double-stranded RNA binding Structural constituent of cytoskeleton Unfolded protein binding	0.93	2.03E-02
MGI:2445114	<i>Pisd</i>	Phosphatidylserine decarboxylase	Lyase activity	0.93	1.94E-02
MGI:96247	<i>Hsp90ab1</i>	Heat shock protein 90 alpha (cytosolic), class B member 1	Unfolded protein binding GTP binding ATP-binding Double-stranded RNA binding Ion channel binding Immune response Negative regulation of neuron apoptotic process	0.90	6.13E-03
MGI:1925017	<i>Ernm</i>	Ermin, ERM-like protein	Actin filament binding	0.90	3.02E-02
MGI:105959	<i>Cox8a</i>	Cytochrome-c oxidase subunit VIIIa	Cytochrome-c oxidase activity	0.88	1.52E-02
MGI:96748	<i>Lamp2</i>	Lysosomal-associated membrane protein 2	Membrane glycoprotein TRNA ligase activity ATP-binding Hemostasis	0.88	2.94E-02
MGI:97748	<i>Ctsa</i>	Cathepsin A	Enzyme activator activity Serine-type carboxypeptidase activity Hydrolase activity	0.86	3.15E-02
MGI:103099	<i>Cox6a1</i>	Cytochrome-c oxidase subunit VIa polypeptide 1	Cytochrome-c oxidase activity	0.85	2.02E-02
MGI:1346074	<i>Fxr2</i>	Fragile X mental retardation, autosomal homolog 2	RNA binding Identical protein binding	0.84	3.11E-02
MGI:99607	<i>Abca1</i>	ATP-binding cassette, sub-family A (ABC1), member 1	Apolipoprotein binding Phospholipid binding Cholesterol binding ATP-binding	0.82	4.37E-02
MGI:88252	<i>Calr</i>	Calreticulin	Iron ion binding Calcium ion binding Hormone binding mRNA binding Regulation of transcription Signal transduction Immune system	0.81	3.02E-02

(Continued)

Table 5 | Continued

ID	Gene name	Gene description	GO biological process annotation/functions	log2 Fold change	Adjusted p-value
MGI:98467	<i>Syp</i>	Synaptophysin	Transporter activity Calcium ion binding Cholesterol binding Syntaxin-1 binding SH2 domain binding Synaptic vesicle maturation Synaptic transmission	0.79	2.74E-02
MGI:98373	<i>Sparc</i>	Secreted acidic cysteine rich glycoprotein	Extracellular matrix binding Calcium ion binding Signal transduction Hemostasis	0.78	4.37E-02
MGI:1096398	<i>Cd81</i>	CD81 antigen	MHC class II protein complex binding Regulation of immune response	0.77	4.93E-02
MGI:1915347	<i>Dynll2</i>	Dynein light chain LC8-type 2	Cytoskeletal protein binding Motor activity	-0.86	2.10E-02
MGI:1277955	<i>Bsn</i>	Bassoon	Metal ion binding Synaptic transmission	-0.87	1.10E-02
MGI:3648294	<i>Tnrc18</i>	Trinucleotide repeat containing 18	DNA binding	-0.87	3.34E-02
MGI:2145310	<i>Rnf44</i>	Ring finger protein 44	Zinc ion binding	-0.89	3.49E-02
MGI:103291	<i>Rai1</i>	Retinoic acid induced 1	Zinc ion binding DNA binding Transcription factor	-0.90	2.82E-02
MGI:1096362	<i>Nrxn2</i>	Neurexin II	Cell adhesion molecule binding Calcium channel regulator activity Metal ion binding Synaptic transmission	-0.90	1.19E-02
MGI:1337000	<i>Rn45s</i>	45S pre-ribosomal 5	Non-coding RNA	-0.90	5.41E-03
MGI:88106	<i>Atp1a2</i>	ATPase, Na ⁺ /K ⁺ transporting, alpha 2 polypeptide	Sodium:potassium-exchanging ATPase activity Metal ion binding Hydrolase activity ATP-binding	-0.90	5.39E-03
MGI:96667	<i>Kcnc1</i>	Potassium voltage -gated channel, shaw-related sub-family, member 1	Rectifier potassium channel activity Voltage-gated ion channel activity Synaptic transmission	-0.92	1.07E-02
MGI:1347488	<i>Foxk1</i>	Forkhead box K1	Transcription regulation Cell differentiation DNA binding Mg-ion binding	-0.94	3.02E-02
MGI:106190	<i>Bcl11a</i>	B cell CLL/lymphoma 11A (zinc finger protein)	B cell differentiation T cell differentiation Regulation of transcription	-0.96	3.73E-02
MGI:1321395	<i>Ltbp4</i>	Latent transforming growth factor beta binding protein 4	Growth factor binding Hormone secretion Regulation of cell differentiation	-0.96	4.59E-02

(Continued)

Table 5 | Continued

ID	Gene name	Gene description	GO biological process annotation/functions	log2 Fold change	Adjusted p-value
MGI:2176606	<i>Scrt1</i>	Scratch homolog 1, zinc finger protein	Transcription regulation	-0.96	2.09E-02
MGI:1925589	<i>Ttyh3</i>	Tweety homolog 3	Chloride channel activity Transmembrane transport	-0.96	7.91E-03
MGI:2444218	<i>Ahd1</i>	AT hook, DNA binding motif, containing 1	DNA binding	-0.97	1.84E-02
MGI:98460	<i>Syn1</i>	Synapsin I	Neurotransmitter secretion Synaptic vesicle transport	-0.98	3.98E-03
MGI:95617	<i>Gabra5</i>	Gamma-aminobutyric acid (GABA) A receptor, subunit alpha 5	GABA-receptor Chloride transport Gamma-aminobutyric acid signaling pathway	-0.99	1.52E-02
MGI:2143099	<i>AI593442</i>	Expressed sequence AI593442	Unclassified	-1.00	4.30E-03
MGI:1346031	<i>Tshz1</i>	Teashirt zinc finger family member 1	Transcription factor DNA binding	-1.00	1.73E-02
MGI:2444817	<i>C530008 M17Rik</i>	RIKEN cDNA C530008M17 gene	Unknown	-1.00	2.26E-02
MGI:2441680	<i>Tmem8b</i>	Transmembrane protein 8B	Cell cycle regulation Cell matrix adhesion	-1.00	2.27E-02
MGI:109169	<i>Epas1</i>	Endothelial PAS domain protein 1	Regulation of transcription Angiogenesis Transcription Signal transduction Cellular stress response	-1.01	6.32E-03
MGI:1351323	<i>Snord33</i>	Small nucleolar RNA, C/D box 33	Unknown	-1.04	4.35E-02
MGI:107363	<i>Stxbp1</i>	Syntaxin binding protein 1	Release of neurotransmitters via syntaxin regulation Vesicle transport Exocytosis Regulation of insulin secretion	-1.04	7.75E-04
MGI:2443847	<i>Sdk2</i>	Sidekick homolog 2	Chemotaxis Protein targeting Cell adhesion	-1.04	2.43E-02
MGI:1919559	<i>Tmem158</i>	Transmembrane protein 158	Ras pathway	-1.06	2.27E-02
MGI:102858	<i>Fosl2</i>	Fos-like antigen 2	Regulation of transcription Cell regulation Fibroblast proliferation	-1.10	1.07E-02
MGI:2686934	<i>Zfx2</i>	Zinc finger homeobox 2	DNA binding Transcriptional factor activity	-1.11	6.32E-03
MGI:96434	<i>Igf2</i>	Insulin-like growth factor 2	Hormone activity Growth factor activity Cell proliferation Regulation of cell cycle Protein metabolism Hemostasis Signal transduction	-1.11	4.47E-03

(Continued)

Table 5 | Continued

ID	Gene name	Gene description	GO biological process annotation/functions	log2 Fold change	Adjusted p-value
MGI:2444034	<i>9530091C08Rik</i>	RIKEN cDNA 9530091C08 gene	Unclassified non-coding RNA gene	-1.14	1.10E-02
MGI:1313277	<i>Vamp2</i>	Vesicle-associated membrane protein 2	Vesicle mediate transport Synaptic vesicle exocytosis Regulation of insulin secretion	-1.14	2.79E-04
MGI:1890616	<i>Scube1</i>	Signal peptide, CUB domain, EGF-like 1	Inflammatory response Endothelial cell differentiation	-1.19	1.28E-03
MGI:2444210	<i>Nr1d1</i>	Nuclear receptor sub-family 1, group D, member 1	Transcription factor Insulin secretion Metabolic processes Inflammatory processes	-1.23	6.34E-04
MGI:2444521	<i>Rnf165</i>	Ring finger protein 165	Zinc ion binding	-1.25	1.05E-02
MGI:1351339	<i>Grm2</i>	Glutamate receptor, metabotropic 2	Synaptic transmission Glutamate secretion	-1.27	2.12E-03
MGI:102703	<i>Gng4</i>	Guanine nucleotide binding protein (G-protein), gamma 4	Signal transduction GTPase activity Hemostasis Synaptic transmission Glucagon response Transmembrane transport of small molecules	-1.42	7.64E-05
MGI:95295	<i>Egr1</i>	Early growth response 1	Transcriptional regulator Immune response T cell differentiation	-1.55	6.15E-07

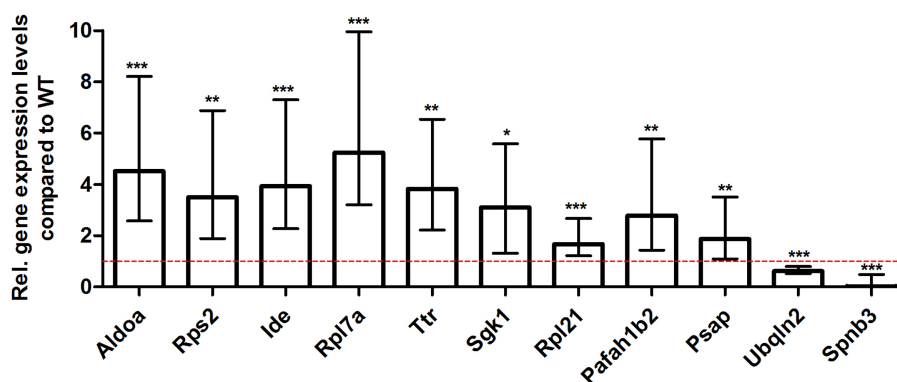
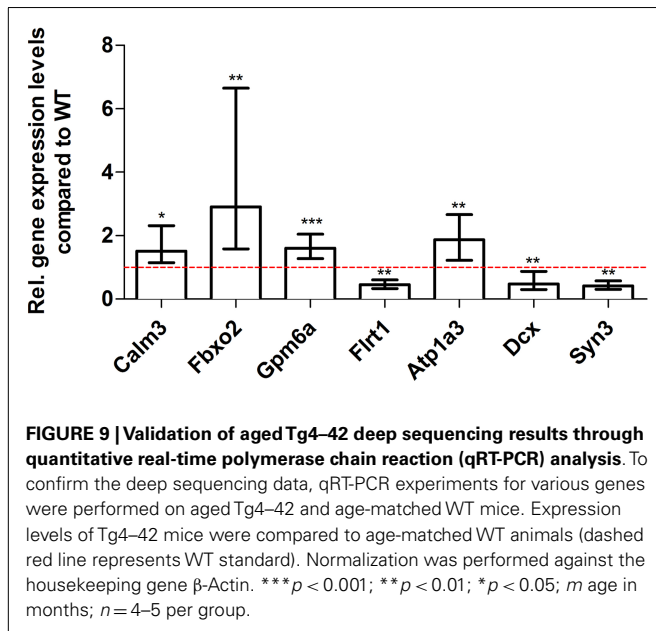
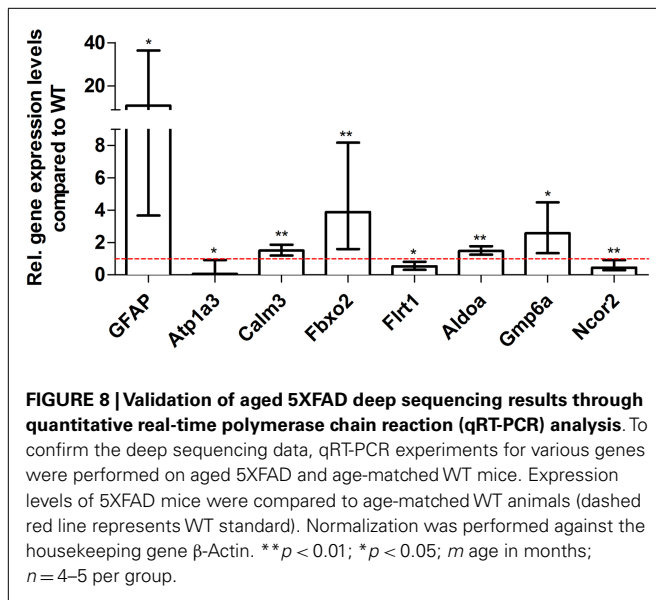


FIGURE 7 | Validation of young 5XFAD deep sequencing results through quantitative real-time polymerase chain reaction (qRT-PCR) analysis. To confirm the deep sequencing data, qRT-PCR experiments for various genes were performed on young 5XFAD and age-matched WT mice. Expression

levels of 5XFAD mice were compared to age-matched WT animals (dashed red line represents WT standard). Normalization was performed against the housekeeping gene β -Actin. *** $p < 0.001$; ** $p < 0.01$; * $p < 0.05$; m age in months; $n = 4-5$ per group.

Another notable down-regulated gene in aged Tg4–42 mice codes for doublecortin (*Dcx*). Doublecortin is a microtubule-associated protein that is expressed in migrating neuronal precursors of the developing CNS and immature neurons (Couillard-Despres et al., 2005). Human DCX is often used as a marker for neurogenesis (Couillard-Despres et al., 2005; Verwer et al., 2007). In AD mouse models expressing mutant forms

of APP or PSEN-1, neurogenesis was found to be impaired. $A\beta$ was found to disrupt neurogenesis in the subventricular zone and the hippocampus in these mice (Haughey et al., 2002a,b). Jin et al. (2004) however described increased levels of doublecortin in the hippocampus of AD patients brains and therefore suggested that neurogenesis is increased in AD hippocampus.



The pathology of AD has recently been linked to the deregulation of cyclin-dependent kinase 5 (CDK5) (Shukla et al., 2012). CDK5 is regulated by the neuron-specific cyclin-related proteins p35 (CDK5R1) and p39 (CDK5R2). Activated CDK5 plays an important role in neurogenesis, synaptic plasticity and neuronal survival (Nikolic et al., 1996; Tan et al., 2003; Shukla et al., 2012). CDK5 phosphorylates tau and the CDK5 complex is involved in posttranslational modification of APP and PSEN (Rademakers et al., 2005). Various neurotoxic events, including oxidative stress and elevated A β levels, result in calpain cleavage of the regulatory proteins p39 and p35. The resulting C-terminal truncated proteins p29 and p25 lead to hyperactivation and mislocalization of CDK5. The introduction of p25 in primary neurons leads to the

Table 6 | Comparison of the two transgenic mouse models 5XFAD and Tg4-42.

Features	5XFAD	Tg4-42
Mutations	APP695 (Swedish, Florida, London) PSEN-1 (M146L and L286V)	None
Genetic background	C57Bl6	C57Bl6
Transient intraneuronal A β	Yes	Yes
Prevalence of A β variants	A β 1-42 > 1-40 > 4-42 > pyroglutamate3-42	only A β 4-42
Plaques	Plaque deposits starting at 3 months	None
Neuron loss	38% loss in cortical layer 5	49% loss in CA1
Gliosis	Yes	Yes
Behavioral deficits	Yes	Yes

deregulation of CDK5 causing among others phosphorylation of tau and neuronal cell death (Cruz and Tsai, 2004; Rademakers et al., 2005). It can be hypothesized that the over-expression of A β 4-42 in Tg4-42 mice stimulates activation of calpain and therefore down-regulation of Cyclin-dependent kinase 5 activator 2.

It is notable that several DEGs in aged Tg4-42 mice have an ion binding function. The proteins ZMIZ2 and ZFP609 bind to zinc ions while Beta-S is an iron ion binding protein. Furthermore, the metal ion binding proteins MLL1, ZFH3, SRRM2, and ATP1A are down-regulated in both aged Tg4-42 and 5XFAD mice. The binding targets zinc and iron, in addition to copper, have been shown to be involved in the pathology of AD. Zinc promotes the aggregation of A β (Watt et al., 2010) and was found to be enriched in AD plaques (Lovell et al., 1998; Leskovjan et al., 2011; Roberts et al., 2012). While the overall Zn level in the aging brain is relatively constant, the zinc transporter ZnT3 has been shown to decrease with age (Roberts et al., 2012). Furthermore, disruption of zinc homeostasis in the brain leads to synaptic and memory deficits (Watt et al., 2010). Aged 5XFAD mice also displayed a variety of DEGs involved in metal binding, for example *Bsn*, *Rnf44*, *Rail1*, *Atp1a2*, and *Rnf165*.

DIFFERENTIALLY EXPRESSED GENES IN AGED 5XFAD MICE

Inflammatory processes

In aged 5XFAD mice 131 genes with significant expression changes were identified. Eighty-seven of these genes were only found to be altered in this mouse line and not in Tg4-42. Compared to aged Tg4-42 mice, a significant larger number of genes were differentially expressed in aged 5XFAD mice.

Recently, Upadhaya et al. (2013) suggested somatic versus neurotic mechanism by which A β may cause neurodegeneration in APP48 and APP23 transgenic mice, respectively. The authors defined the somatic type of neurodegeneration as intraneuronal accumulations of A β that are produced independent of APP.

In contrast to the APP48 model, the Tg4–42 mice did not develop such a dendritic pathology (Bouter et al., 2013). This may be due to the different signal peptides used in APP48 (preproenkephalin) and Tg4–42 (thyrotropin-releasing hormone). The signal peptide of Tg4–42 ensures the routing through the secretory pathway allowing the release of the peptide from neurons.

The neuritic type of neurodegeneration linking APP-derived extra- and intracellular A β aggregation may be similar between APP23 and 5XFAD mice. Hence, the DEGs observed in 5XFAD and Tg4–42 mice could be partly explained by the different mechanism by which A β causes neurodegeneration in these two models.

A large number of DEGs is involved in regulation of immune system processes and inflammation. The respective transcripts are involved among others in adaptive immune response, regulation, and activation of immune response as well as immune system development. Inflammatory processes in the brain are a well-described feature of AD. It has been shown that plaque deposition in AD brains is associated with chronic inflammation characterized by increased inflammatory cytokine expression and activation of microglia, astrocytes, and complement factors (Akiyama et al., 2000). Inflammation is thought to be a downstream process appearing after A β plaques, NFT, and neuron degeneration (Arnaud et al., 2006). 5XFAD mice display distinct neuroinflammatory features. The number of reactive astrocytes and microglia increases proportionally to the amyloid burden in this mouse line (Oakley et al., 2006; Kalinin et al., 2009).

5XFAD mice also show a dramatic increase in A β 42 in comparison to A β 40. This results in an early pathology onset with plaque deposition seen as early as 3 months of age. The plaque pathology increases dramatically in an age-dependent manner (Oakley et al., 2006; Jawhar et al., 2010). Aggregation of A β results in activated microglia and induces the production of reactive-oxygen species, pro-inflammatory cytokines, chemokines, and prostaglandines leading to degenerative changes in neurons (Akiyama et al., 2000).

A large number of DEGs in aged 5XFAD mice have a role in inflammatory pathways (including *Scube1* and *Nr1d1*). Strikingly, four genes of the complement system (*C4b*, *C1qa*, *C1qb*, and *C1qc*) are highly up-regulated in 12-month-old 5XFAD mice. Complement activation is a major inflammatory process and is thought to be activated in AD by the interaction of complement proteins with the aggregated forms of A β and tau (Rogers et al., 1992; Shen et al., 2001).

Notably, five genes, encoding the cysteine proteases Cathepsin B, Cathepsin L, Cathepsin S, and Cathepsin Z as well as the aspartyl protease Cathepsin D, were up-regulated in aged 5XFAD mice. Cathepsin D is a lysosomal enzyme found in neuritic plaques and is considered to be involved in APP processing (Schuur et al., 2011). Cataldo et al. (1995) showed an up-regulation of Cathepsin D mRNA in the pyramidal neurons of AD brains. The cysteine protease Cathepsin B has been proposed as an alternative candidate β -secretase in the regulated secretory pathway of neurons, where it produces A β by cleavage of the WT β -secretase site of APP (Hook et al., 2009; Wang et al., 2012). Hook et al. (2009) demonstrated that deletion of Cathepsin B in a hAPPwt transgenic mouse model significantly reduced the levels of A β 40 and A β 42. Therefore, Cathepsin B might be a valid target for developing inhibitors to lower brain A β levels in AD patients.

Another interesting gene that showed an up-regulated expression in aged 5XFAD mice is clusterin (*Clu*) also known as apolipoprotein J. Clusterin is a chaperone glycoprotein that affects many cellular processes, including inflammation. Clusterin is elevated in AD affected brain regions and CSF from AD patients (Lidström et al., 1998; Nilsseld et al., 2006). Furthermore, it was found to be associated with AD in several large genome-wide association studies (GWAS) (Harold et al., 2009; Lambert et al., 2009; Carrasquillo et al., 2010). Recent studies suggest that Clusterin contributes to the pathology to AD through various pathways, including lipid metabolism, neuroinflammation, and apoptosis. Interestingly, it is reported to increase A β aggregation as well as A β clearance (Yu and Tan, 2012).

It should be noted that *Inpp5d* RNA was found to be differentially expressed in 5XFAD mice. This gene was recently described as a new locus for AD in a GWAS (Lambert et al., 2013). *Inpp5d* encodes a member of the inositol polyphosphate-5-phosphatase family of enzymes involved in second messenger signaling in myeloid cells. INPP5D influences pathways that are associated with cell proliferation and inflammatory responses (Medway and Morgan, 2014).

EVIDENCE FOR DIVERSE MOLECULAR PATHWAYS

In addition to genes involved in inflammatory processes, DEGs in aged 5XFAD mice were also involved in cell communication and system development, signal transduction, synaptic transmission as well as regulation of gene expression and transcription.

We observed significant transcriptional changes of genes with synaptic function in aged 5XFAD mice. For instance, the gene products of *Bsn*, *Nrxn2*, *Kcnc1*, *Grm2*, and *Gng4* all play a role in synaptic transmission and are down-regulated in 12-month-old 5XFAD mice. *Syn1*, the gene encoding Synapsin1, a neuronal phosphoprotein associated with the cytoplasmic surface of synaptic vesicles, is significantly down-regulated in aged 5XFAD mice. It is involved in synapse formation and promotion of neurotransmitter release (Südhof, 1990; Jaffrey et al., 2002). Qin et al. (2004) showed that synapsin levels were also significantly decreased in the CA1 and the dentate gyrus in AD patients.

Wirz et al. (2013) studied the genome-wide gene expression of another AD double transgenic APP/PS1 mouse model using microarrays. A vast range of genes was altered in these APP/PS1 Δ Ex9 mice that are involved in immune response and inflammation. In contrast to our observations in 5XFAD mice, no changes in the expression of genes involved in synaptic plasticity or transmission were found. However, in AD patients dominant gene expression changes concerning synaptic plasticity or transmission were recently described in a genome-wide gene expression study of the prefrontal cortex (Bossers et al., 2010). It can be argued that deep sequencing and the use of 5XFAD mice are more informative and better suited to identify the expression changes in a model system of AD.

LIMITATIONS OF THE STUDY

Finally, it can be stated that RNA-Seq is a powerful technique to analyze the expression profiles in AD mice. The detection of hundreds of DEGs may offer a new perspective on the biological processes underlying the pathology of AD. However, even though

there is a strong correlation between gene expression levels and abundances of the respectively corresponding proteins in mammalian cells (Lundberg et al., 2010), it has to be kept in mind that proteins, rather than mRNAs, are the main mediators of physiological processes and that there is a considerable body of data that suggests a major role for post-transcriptional processes in controlling protein abundances (Vogel and Marcotte, 2012).

While investigating the role of DEGs on the protein level is beyond the scope of this study, we believe that the presented dataset will provide an important source of information for the validation in both mouse and human tissue in independent studies. A wide range of detected genes were previously shown to be regulated in AD, however, a variety of DEGs in the studied mouse models were not previously associated with AD in humans. It remains to be seen if these genes are also regulated in AD cases.

In agreement with the German guidelines for animal care all animals were sacrificed by CO₂ anesthesia. This treatment may lead to prefinal hypoxia in both the transgenic as well as in the control wildtype mice. However, it cannot be ruled out that hypoxia has distinct effects on transgenic mice inducing a different set of DEGs.

CONCLUSION

In conclusion, we could (1) validate the Tg4–42 model expressing only A β _{4–42} as a valuable model for AD. The comparison with 5XFAD, an established plaque-developing AD mouse model, revealed a remarkable overlap in the molecular profile with the Tg4–42 model. Although the 5XFAD produces also A β _{4–42}, A β _{1–42} is more abundant followed A β _{1–40} and pyroglutamated and non-pyroglutamated A β _{3–42}. The jointly DEGs might indicate common pathways that are involved in the learning and memory decline apparent at 12 months of age in both transgenic models. (2) The pool of genes that showed differential expression exclusively in Tg4–42 is only associated to soluble A β _{4–42} as no extracellular plaques or other A β variants are found in this model. In addition, the robust CA1 neuron loss could also contribute to the differential expression profile. (3) As most of the genes with expression levels exclusively altered in 5XFAD mice belong to inflammation-associated pathways, we conclude that the majority is not associated with neuron loss and memory decline. (4) As expected, the deep sequencing approach identified a plethora of genes that have so far not been linked to AD, which might opens up new avenues of research into the etiology of this devastating neurodegenerative disorder.

AUTHOR CONTRIBUTIONS

Yvonne Bouter wrote the manuscript, contributed to experimental design, analyzed data and performed experiments. Tim Kacprowski analyzed data. Robert Weissmann performed experiments and analyzed data. Katharina Dietrich, Henning Borgers, Andreas Brauß, Christian Sperling and Lars R. Jensen performed experiments. Oliver Wirths, Mario Albrecht and Andreas W. Kuss contributed to experimental design. Thomas A. Bayer analyzed data and supervised experimental design and the entire project.

ACKNOWLEDGMENTS

We thank Petra Tucholla for excellent technical help. Tim Kacprowski's position is funded by the Federal Ministry of Cultural

Affairs of the Federal State of Mecklenburg-West Pomerania through the GANI_MED (Greifswald Approach to Individualized Medicine) project (03IS2061A). We acknowledge support by the Open Access Publication Funds of the Göttingen University. Mario Albrecht is supported by the projects GANI_MED and BioTechMed-Graz.

REFERENCES

- Akiyama, H., Barger, S., Barnum, S., Bradt, B., Bauer, J., Cole, G. M., et al. (2000). Inflammation and Alzheimer's disease. *Neurobiol. Aging* 21, 383–421. doi:10.1016/S0197-4580(00)00124-X
- Altar, A. C., Vawter, M. P., and Ginsberg, S. D. (2009). Target identification for CNS diseases by transcriptional profiling. *Neuropsychopharmacology* 34, 18–54. doi:10.1038/npp.2008.172
- Alzheimer's Association. (2012). 2012 Alzheimer's disease facts and figures. *Alzheimers Dement.* 8, 131–168. doi:10.1016/j.jalz.2012.02.001
- Anders, S., and Huber, W. (2010). Differential expression analysis for sequence count data. *Genome Biol.* 11, R106. doi:10.1186/gb-2010-11-10-r106
- Arnau, L., Robakis, N. K., and Figueiredo-Pereira, M. E. (2006). It may take inflammation, phosphorylation and ubiquitination to 'tangle' in Alzheimer's disease. *Neurodegener. Dis.* 3, 313–319. doi:10.1159/000095638
- Ashburner, M., Ball, C. A., Blake, J. A., Botstein, D., Butler, H., Cherry, J. M., et al. (2000). Gene ontology: tool for the unification of biology. The gene ontology consortium. *Nat. Genet.* 25, 25–29. doi:10.1038/75556
- Bast, T., Zhang, W.-N., and Feldon, J. (2003). Dorsal hippocampus and classical fear conditioning to tone and context in rats: effects of local NMDA-receptor blockade and stimulation. *Hippocampus* 13, 657–675. doi:10.1002/hipo.10115
- Benilova, I., Karran, E., and DeStrooper, B. (2012). The toxic A β oligomer and Alzheimer's disease: an emperor in need of clothes. *Nat. Neurosci.* 15, 349–357. doi:10.1038/nn.3028
- Bertram, L., and Tanzi, R. E. (2001). Dancing in the dark? The status of late-onset Alzheimer's disease genetics. *J. Mol. Neurosci.* 17, 127–136. doi:10.1385/JMN:17:2:127
- Blennow, K., deLeon, M. J., and Zetterberg, H. (2006). Alzheimer's disease. *Lancet* 368, 387–403. doi:10.1016/S0140-6736(06)69113-7
- Bossers, K., Wirz, K. T. S., Meerhoff, G. F., Essing, A. H. W., van Dongen, J. W., Houba, P., et al. (2010). Concerted changes in transcripts in the prefrontal cortex precede neuropathology in Alzheimer's disease. *Brain* 133, 3699–3723. doi:10.1093/brain/awq258
- Bouter, Y., Dietrich, K., Wittnam, J. L., Rezaei-Ghaleh, N., Pillot, T., Papot-Couturier, S., et al. (2013). N-truncated amyloid β (A β) 4–42 forms stable aggregates and induces acute and long-lasting behavioral deficits. *Acta Neuropathol.* 126, 189–205. doi:10.1007/s00401-013-1129-2
- Breyhan, H., Wirths, O., Duan, K., Marcello, A., Rettig, J., and Bayer, T. A. (2009). APP/PS1KI bigenic mice develop early synaptic deficits and hippocampus atrophy. *Acta Neuropathol.* 117, 677–685. doi:10.1007/s00401-009-0539-7
- Carrasquillo, M. M., Belbin, O., Hunter, T. A., Ma, L., Biscoglio, G. D., Zou, F., et al. (2010). Replication of CLU, CR1, and PICALM associations with Alzheimer disease. *Arch. Neurol.* 67, 961–964. doi:10.1001/archneurol.2010.147
- Carrette, O., Demalte, I., Scherl, A., Yalkinoglu, O., Corthals, G., Burkhard, P., et al. (2003). A panel of cerebrospinal fluid potential biomarkers for the diagnosis of Alzheimer's disease. *Proteomics* 3, 1486–1494. doi:10.1002/pmic.200300470
- Casas, C., Sergeant, N., Itier, J.-M., Blanchard, V., Wirths, O., van der Kolk, N., et al. (2004). Massive CA1/2 neuronal loss with intraneuronal and N-terminal truncated Abeta42 accumulation in a novel Alzheimer transgenic model. *Am. J. Pathol.* 165, 1289–1300. doi:10.1016/S0002-9440(10)63388-3
- Cataldo, A. M., Barnett, J. L., Berman, S. A., Li, J., Quarless, S., Bursztajn, S., et al. (1995). Gene expression and cellular content of cathepsin D in Alzheimer's disease brain: evidence for early up-regulation of the endosomal-lysosomal system. *Neuron* 14, 671–680. doi:10.1016/0896-6273(95)90324-0
- Chen, G., Chen, K. S., Knox, J., Inglis, J., Bernard, A., Martin, S. J., et al. (2000). A learning deficit related to age and beta-amyloid plaques in a mouse model of Alzheimer's disease. *Nature* 408, 975–979. doi:10.1038/35050103
- Cheng, L., Quek, C. Y. J., Sun, X., Bellingham, S. A., and Hill, A. F. (2013). The detection of microRNA associated with Alzheimer's disease in biological fluids using next-generation sequencing technologies. *Front. Genet.* 4:150. doi:10.3389/fgene.2013.00150

- Choi, J. W., Kang, S. M., Lee, Y., Hong, S. H., Sanek, N. A., Young, W. S., et al. (2013). MicroRNA profiling in the mouse hypothalamus reveals oxytocin-regulating microRNA. *J. Neurochem.* 126, 331–337. doi:10.1111/jnc.12308
- Christensen, D. Z., Bayer, T. A., and Wirths, O. (2010). Intracellular A β triggers neuron loss in the cholinergic system of the APP/PS1KI mouse model of Alzheimer's disease. *Neurobiol. Aging* 31, 1153–1163. doi:10.1016/j.neurobiolaging.2008.07.022
- Christensen, D. Z., Kraus, S. L., Flohr, A., Cotel, M.-C., Wirths, O., and Bayer, T. A. (2008). Transient intraneuronal A beta rather than extracellular plaque pathology correlates with neuron loss in the frontal cortex of APP/PS1KI mice. *Acta Neuropathol.* 116, 647–655. doi:10.1007/s00401-008-0451-6
- Cocco, C., D'Amato, F., Noli, B., Ledda, A., Brancia, C., Bongioanni, P., et al. (2010). Distribution of VGF peptides in the human cortex and their selective changes in Parkinson's and Alzheimer's diseases. *J. Anat.* 217, 683–693. doi:10.1111/j.1469-7580.2010.01309.x
- Couillard-Despres, S., Winner, B., Schaubek, S., Aigner, R., Vroemen, M., Weidner, N., et al. (2005). Doublecortin expression levels in adult brain reflect neurogenesis. *Eur. J. Neurosci.* 21, 1–14. doi:10.1111/j.1460-9568.2004.03813.x
- Courtney, E., Kornfeld, S., Janitz, K., and Janitz, M. (2010). Transcriptome profiling in neurodegenerative disease. *J. Neurosci. Methods* 193, 189–202. doi:10.1016/j.jneumeth.2010.08.018
- Cruz, J. C., and Tsai, L.-H. (2004). Cdk5 deregulation in the pathogenesis of Alzheimer's disease. *Trends Mol. Med.* 10, 452–458. doi:10.1016/j.molmed.2004.07.001
- Delacourte, A. (1990). General and dramatic glial reaction in Alzheimer brains. *Neurology* 40, 33–37. doi:10.1212/WNL.40.1.33
- Dickey, C. A., Loring, J. F., Montgomery, J., Gordon, M. N., Eastman, P. S., and Morgan, D. (2003). Selectively reduced expression of synaptic plasticity-related genes in amyloid precursor protein + presenilin-1 transgenic mice. *J. Neurosci.* 23, 5219–5226.
- España, J., Giménez-Llort, L., Valero, J., Miñano, A., Rábano, A., Rodríguez-Alvarez, J., et al. (2010). Intraneuronal beta-amyloid accumulation in the amygdala enhances fear and anxiety in Alzheimer's disease transgenic mice. *Biol. Psychiatry* 67, 513–521. doi:10.1016/j.biopsych.2009.06.015
- Farris, W., Mansourian, S., Chang, Y., Lindsley, L., Eckman, E. A., Frosch, M. P., et al. (2003). Insulin-degrading enzyme regulates the levels of insulin, amyloid beta-protein, and the beta-amyloid precursor protein intracellular domain in vivo. *Proc. Natl. Acad. Sci. U.S.A.* 100, 4162–4167. doi:10.1073/pnas.0230450100
- George, A. J., Gordon, L., Beissbarth, T., Koukoulas, I., Holsinger, R. M., Perreau, V., et al. (2010). A serial analysis of gene expression profile of the Alzheimer's disease Tg2576 mouse model. *Neurotox. Res.* 17, 360–379. doi:10.1007/s12640-009-9112-3
- Glaser, S., Schaft, J., Lubitz, S., Vintersten, K., van der Hoeven, F., Tufeland, K. R., et al. (2006). Multiple epigenetic maintenance factors implicated by the loss of Mll2 in mouse development. *Development* 133, 1423–1432. doi:10.1242/dev.02302
- Haass, C., and Selkoe, D. J. (2007). Soluble protein oligomers in neurodegeneration: lessons from the Alzheimer's amyloid beta-peptide. *Nat. Rev. Mol. Cell Biol.* 8, 101–112. doi:10.1038/nrm2101
- Hardy, J., and Allsop, D. (1991). Amyloid deposition as the central event in the aetiology of Alzheimer's disease. *Trends Pharmacol. Sci.* 12, 383–388. doi:10.1016/0165-6147(91)90609-V
- Harold, D., Abraham, R., Hollingworth, P., Sims, R., Gerrish, A., Hamshere, M. L., et al. (2009). Genome-wide association study identifies variants at CLU and PICALM associated with Alzheimer's disease. *Nat. Genet.* 41, 1088–1093. doi:10.1038/ng.440
- Haughey, N. J., Liu, D., Nath, A., Borchard, A. C., and Mattson, M. P. (2002a). Disruption of neurogenesis in the subventricular zone of adult mice, and in human cortical neuronal precursor cells in culture, by amyloid beta-peptide: implications for the pathogenesis of Alzheimer's disease. *Neuromolecular Med.* 1, 125–135. doi:10.1385/NMM:1:2:125
- Haughey, N. J., Nath, A., Chan, S. L., Borchard, A. C., Rao, M. S., and Mattson, M. P. (2002b). Disruption of neurogenesis by amyloid beta-peptide, and perturbed neural progenitor cell homeostasis, in models of Alzheimer's disease. *J. Neurochem.* 83, 1509–1524. doi:10.1046/j.1471-4159.2002.01267.x
- Haupt, C., Leppert, J., Rönicke, R., Meinhardt, J., Yadav, J. K., Ramachandran, R., et al. (2012). Structural basis of β -amyloid-dependent synaptic dysfunctions. *Angew. Chem. Int. Ed. Engl.* 51, 1576–1579. doi:10.1002/anie.201105638
- Hillmann, A., Hahn, S., Schilling, S., Hoffmann, T., Demuth, H.-U., Bulic, B., et al. (2012). No improvement after chronic ibuprofen treatment in the 5XFAD mouse model of Alzheimer's disease. *Neurobiol. Aging* 33, e39–e50. doi:10.1016/j.neurobiolaging.2011.08.006
- Hirokawa, N., Niwa, S., and Tanaka, Y. (2010). Molecular motors in neurons: transport mechanisms and roles in brain function, development, and disease. *Neuron* 68, 610–638. doi:10.1016/j.neuron.2010.09.039
- Hirokawa, N., Noda, Y., Tanaka, Y., and Niwa, S. (2009). Kinesin superfamily motor proteins and intracellular transport. *Nat. Rev. Mol. Cell Biol.* 10, 682–696. doi:10.1038/nrm2774
- Hook, V. Y., Kindy, M., Reinheckel, T., Peters, C., and Hook, G. (2009). Genetic cathepsin B deficiency reduces beta-amyloid in transgenic mice expressing human wild-type amyloid precursor protein. *Biochem. Biophys. Res. Commun.* 386, 284–288. doi:10.1016/j.bbrc.2009.05.131
- Jaffrey, S. R., Benfenati, F., Snowman, A. M., Czernik, A. J., and Snyder, S. H. (2002). Neuronal nitric-oxide synthase localization mediated by a ternary complex with synapsin and CAPON. *Proc. Natl. Acad. Sci. U.S.A.* 99, 3199–3204. doi:10.1073/pnas.261705799
- Jahn, H., Wittke, S., Zürgbig, P., Raedler, T. J., Arlt, S., Kellmann, M., et al. (2011). Peptide fingerprinting of Alzheimer's disease in cerebrospinal fluid: identification and prospective evaluation of new synaptic biomarkers. *PLoS ONE* 6:e26540. doi:10.1371/journal.pone.0026540
- Jawhar, S., Trawicka, A., Jenneckens, C., Bayer, T. A., and Wirths, O. (2010). Motor deficits, neuron loss, and reduced anxiety coinciding with axonal degeneration and intraneuronal A β aggregation in the 5XFAD mouse model of Alzheimer's disease. *Neurobiol. Aging* 33, e29–e40. doi:10.1016/j.neurobiolaging.2010.05.027
- Jawhar, S., Wirths, O., and Bayer, T. A. (2011). Pyroglutamate amyloid- β (A β): a hatchet man in Alzheimer disease. *J. Biol. Chem.* 286, 38825–38832. doi:10.1074/jbc.R111.288308
- Jin, K., Peel, A. L., Mao, X. O., Xie, L., Cottrell, B. A., Henshall, D. C., et al. (2004). Increased hippocampal neurogenesis in Alzheimer's disease. *Proc. Natl. Acad. Sci. U.S.A.* 101, 343–347. doi:10.1073/pnas.2634794100
- Kalinin, S., Richardson, J. C., and Feinstein, D. L. (2009). A PPAR δ agonist reduces amyloid burden and brain inflammation in a transgenic mouse model of Alzheimer's disease. *Curr. Alzheimer Res.* 6, 431–437. doi:10.2174/156720509789207949
- Kanekiyo, T., Cirrito, J. R., Liu, C.-C., Shinohara, M., Li, J., Schuler, D. R., et al. (2013). Neuronal clearance of amyloid- β by endocytic receptor LRP1. *J. Neurosci.* 33, 19276–19283. doi:10.1523/JNEUROSCI.3487-13.2013
- Kerimoglu, C., Agis-Balboa, R. C., Kranz, A., Stilling, R., Bahari-Javan, S., Benito-Garagorri, E., et al. (2013). Histone-methyltransferase MLL2 (KMT2B) is required for memory formation in mice. *J. Neurosci.* 33, 3452–3464. doi:10.1523/JNEUROSCI.3356-12.2013
- Kishimoto, Y., Higashihara, E., Fukuta, A., Nagao, A., and Kirino, Y. (2013). Early impairment in a water-finding test in a longitudinal study of the Tg2576 mouse model of Alzheimer's disease. *Brain Res.* 1491, 117–126. doi:10.1016/j.brainres.2012.10.066
- Klein, W. L. (2002). A β toxicity in Alzheimer's disease: globular oligomers (ADDLs) as new vaccine and drug targets. *Neurochem. Int.* 41, 345–352. doi:10.1016/S0197-0186(02)00050-5
- Ko, H. S., Uehara, T., Tsuruma, K., and Nomura, Y. (2004). Ubiquitin interacts with ubiquitylated proteins and proteasome through its ubiquitin-associated and ubiquitin-like domains. *FEBS Lett.* 566, 110–114. doi:10.1016/j.febslet.2004.04.031
- Kondo, M., Takei, Y., and Hirokawa, N. (2012). Motor protein KIF1A is essential for hippocampal synaptogenesis and learning enhancement in an enriched environment. *Neuron* 73, 743–757. doi:10.1016/j.neuron.2011.12.020
- Lambert, J.-C., Heath, S., Even, G., Campion, D., Sleegers, K., Hiltunen, M., et al. (2009). Genome-wide association study identifies variants at CLU and CR1 associated with Alzheimer's disease. *Nat. Genet.* 41, 1094–1099. doi:10.1038/ng.439
- Lambert, J.-C., Ibrahim-Verbaas, C. A., Harold, D., Naj, A. C., Sims, R., Bellenguez, C., et al. (2013). Meta-analysis of 74,046 individuals identifies 11 new susceptibility loci for Alzheimer's disease. *Nat. Genet.* 45, 1452–1458. doi:10.1038/ng.2802
- Leskova, A. C., Kretlow, A., Lanzirrotti, A., Barrea, R., Vogt, S., and Miller, L. M. (2011). Increased brain iron coincides with early plaque formation in a mouse model of Alzheimer's disease. *Neuroimage* 55, 32–38. doi:10.1016/j.neuroimage.2010.11.073

- Lesné, S. E., Sherman, M. A., Grant, M., Kuskowski, M., Schneider, J. A., Bennett, D. A., et al. (2013). Brain amyloid- β oligomers in ageing and Alzheimer's disease. *Brain* 136, 1383–1398. doi:10.1093/brain/awt062
- Li, X., and Buxbaum, J. N. (2011). Transthyretin and the brain re-visited: is neuronal synthesis of transthyretin protective in Alzheimer's disease? *Mol. Neurodegener.* 6, 79. doi:10.1186/1750-1326-6-79
- Lidström, A. M., Bogdanovic, N., Hesse, C., Volkman, I., Davidsson, P., and Blennow, K. (1998). Clusterin (apolipoprotein J) protein levels are increased in hippocampus and in frontal cortex in Alzheimer's disease. *Exp. Neurol.* 154, 511–521. doi:10.1006/exnr.1998.6892
- Lovell, M. A., Robertson, J. D., Teesdale, W. J., Campbell, J. L., and Markesbery, W. R. (1998). Copper, iron and zinc in Alzheimer's disease senile plaques. *J. Neurol. Sci.* 158, 47–52. doi:10.1016/S0022-510X(98)00092-6
- Lundberg, E., Fagerberg, L., Klevebring, D., Matic, I., Geiger, T., Cox, J., et al. (2010). Defining the transcriptome and proteome in three functionally different human cell lines. *Mol. Syst. Biol.* 6, 450. doi:10.1038/msb.2010.106
- Masters, C. L., Simms, G., Weinman, N. A., Multhaup, G., McDonald, B. L., and Beyreuther, K. (1985). Amyloid plaque core protein in Alzheimer disease and Down syndrome. *Proc. Natl. Acad. Sci. U.S.A.* 82, 4245–4249. doi:10.1073/pnas.82.12.4245
- McLean, C. A., Cherny, R. A., Fraser, F. W., Fuller, S. J., Smith, M. J., Beyreuther, K., et al. (1999). Soluble pool of Abeta amyloid as a determinant of severity of neurodegeneration in Alzheimer's disease. *Ann. Neurol.* 46, 860–866. doi:10.1002/1531-8249(199912)46:6<860::AID-ANA8>3.0.CO;2-M
- Medway, C., and Morgan, K. (2014). Review: the genetics of Alzheimer's disease; putting flesh on the bones. *Neuropathol. Appl. Neurobiol.* 40, 97–105. doi:10.1111/nan.12101
- Miller, D. L., Papayannopoulos, I. A., Styles, J., Bobin, S. A., Lin, Y. Y., Biemann, K., et al. (1993). Peptide compositions of the cerebrovascular and senile plaque core amyloid deposits of Alzheimer's disease. *Arch. Biochem. Biophys.* 301, 41–52. doi:10.1006/abbi.1993.1112
- Miners, J. S., Baig, S., Tayler, H., Kehoe, P. G., and Love, S. (2009). Neprilysin and insulin-degrading enzyme levels are increased in Alzheimer disease in relation to disease severity. *J. Neuropathol. Exp. Neurol.* 68, 902–914. doi:10.1097/NEN.0b013e3181afe475
- Moechars, D., Dewachter, I., Lorent, K., Reversé, D., Baekelandt, V., Naidu, A., et al. (1999). Early phenotypic changes in transgenic mice that overexpress different mutants of amyloid precursor protein in brain. *J. Biol. Chem.* 274, 6483–6492. doi:10.1074/jbc.274.10.6483
- Moechars, D., Lorent, K., Strooper, B., Dewachter, I., and van Leuven, F. (1996). Expression in brain of amyloid precursor protein mutated in the alpha-secretase site causes disturbed behavior, neuronal degeneration and premature death in transgenic mice. *EMBO J.* 15, 1265–1274.
- Morris, R. (1984). Developments of a water-maze procedure for studying spatial learning in the rat. *J. Neurosci. Methods* 11, 47–60. doi:10.1016/0165-0270(84)90007-4
- Nagalakshmi, U., Wang, Z., Waern, K., Shou, C., Raha, D., Gerstein, M., et al. (2008). The transcriptional landscape of the yeast genome defined by RNA sequencing. *Science* 320, 1344–1349. doi:10.1126/science.1158441
- Näslund, J., Haroutunian, V., Mohs, R., Davis, K. L., Davies, P., Greengard, P., et al. (2000). Correlation between elevated levels of amyloid beta-peptide in the brain and cognitive decline. *JAMA* 283, 1571–1577. doi:10.1001/jama.283.12.1571
- Nikolic, M., Dudek, H., Kwon, Y. T., Ramos, Y. F., and Tsai, L. H. (1996). The cdk5/p35 kinase is essential for neurite outgrowth during neuronal differentiation. *Genes Dev.* 10, 816–825. doi:10.1101/gad.10.7.816
- Nilselid, A.-M., Davidsson, P., Nägga, K., Andreasen, N., Fredman, P., and Blennow, K. (2006). Clusterin in cerebrospinal fluid: analysis of carbohydrates and quantification of native and glycosylated forms. *Neurochem. Int.* 48, 718–728. doi:10.1016/j.neuint.2005.12.005
- Oakley, H., Cole, S. L., Logan, S., Maus, E., Shao, P., Craft, J., et al. (2006). Intraneuronal beta-amyloid aggregates, neurodegeneration, and neuron loss in transgenic mice with five familial Alzheimer's disease mutations: potential factors in amyloid plaque formation. *J. Neurosci.* 26, 10129–10140. doi:10.1523/JNEUROSCI.1202-06.2006
- Ohno, M. (2009). Failures to reconsolidate memory in a mouse model of Alzheimer's disease. *Neurobiol. Learn. Mem.* 92, 455–459. doi:10.1016/j.nlm.2009.05.001
- Pfaffl, M. W., Horgan, G. W., and Dempfle, L. (2002). Relative expression software tool (REST) for group-wise comparison and statistical analysis of relative expression results in real-time PCR. *Nucleic Acids Res.* 30, e36. doi:10.1093/nar/30.9.e36
- Pham, E., Crews, L., Ubhi, K., Hansen, L., Adame, A., Cartier, A., et al. (2010). Progressive accumulation of amyloid-beta oligomers in Alzheimer's disease and in amyloid precursor protein transgenic mice is accompanied by selective alterations in synaptic scaffold proteins. *FEBS J.* 277, 3051–3067. doi:10.1111/j.1742-4658.2010.07719.x
- Phillips, R. G., and LeDoux, J. E. (1992). Differential contribution of amygdala and hippocampus to cued and contextual fear conditioning. *Behav. Neurosci.* 106, 274–285. doi:10.1037/0735-7044.106.2.274
- Portelius, E., Bogdanovic, N., Gustavsson, M. K., Volkman, I., Brinkmalm, G., Zetterberg, H., et al. (2010). Mass spectrometric characterization of brain amyloid beta isoform signatures in familial and sporadic Alzheimer's disease. *Acta Neuropathol.* 120, 185–193. doi:10.1007/s00401-010-0690-1
- Prelli, F., Castañó, E., Glenner, G. G., and Frangione, B. (1988). Differences between vascular and plaque core amyloid in Alzheimer's disease. *J. Neurochem.* 51, 648–651. doi:10.1111/j.1471-4159.1988.tb01087.x
- Price, J. L., and Morris, J. C. (1999). Tangles and plaques in nondemented aging and "preclinical" Alzheimer's disease. *Ann. Neurol.* 45, 358–368. doi:10.1002/1531-8249(199903)45:3<358::AID-ANA12>3.0.CO;2-X
- Qin, S., Hu, X.-Y., Xu, H., and Zhou, J.-N. (2004). Regional alteration of synapsin I in the hippocampal formation of Alzheimer's disease patients. *Acta Neuropathol.* 107, 209–215. doi:10.1007/s00401-003-0800-4
- Rademakers, R., Sleegers, K., Theuns, J., van den Broeck, M., Bel Kacem, S., Nilsson, L.-G., et al. (2005). Association of cyclin-dependent kinase 5 and neuronal activators p35 and p39 complex in early-onset Alzheimer's disease. *Neurobiol. Aging* 26, 1145–1151. doi:10.1016/j.neurobiolaging.2004.10.003
- Risso, D., Schwartz, K., Sherlock, G., and Dudoit, S. (2011). GC-content normalization for RNA-Seq data. *BMC Bioinformatics* 12:480. doi:10.1186/1471-2105-12-480
- Roberts, B. R., Ryan, T. M., Bush, A. I., Masters, C. L., and Duce, J. A. (2012). The role of metallobiology and amyloid- β peptides in Alzheimer's disease. *J. Neurochem.* 120(Suppl. 1), 149–166. doi:10.1111/j.1471-4159.2011.07500.x
- Rogers, J., Cooper, N. R., Webster, S., Schultz, J., McGeer, P. L., Styren, S. D., et al. (1992). Complement activation by beta-amyloid in Alzheimer disease. *Proc. Natl. Acad. Sci. U.S.A.* 89, 10016–10020. doi:10.1073/pnas.89.21.10016
- Roychoudhuri, R., Yang, M., Hoshi, M. M., and Teplow, D. B. (2009). Amyloid beta-protein assembly and Alzheimer disease. *J. Biol. Chem.* 284, 4749–4753. doi:10.1074/jbc.R800036200
- Schmitz, C., Rutten, B. P. F., Pielen, A., Schäfer, S., Wirths, O., Tremp, G., et al. (2004). Hippocampal neuron loss exceeds amyloid plaque load in a transgenic mouse model of Alzheimer's disease. *Am. J. Pathol.* 164, 1495–1502. doi:10.1016/S0002-9440(10)63235-X
- Schuur, M., Ikram, M. A., van Swieten, J. C., Isaacs, A., Vergeer-Drop, J. M., Hofman, A., et al. (2011). Cathepsin D gene and the risk of Alzheimer's disease: a population-based study and meta-analysis. *Neurobiol. Aging* 32, 1607–1614. doi:10.1016/j.neurobiolaging.2009.10.011
- Selkoe, D. J. (1998). The cell biology of beta-amyloid precursor protein and presenilin in Alzheimer's disease. *Trends Cell Biol.* 8, 447–453. doi:10.1016/S0962-8924(98)01363-4
- Selkoe, D. J. (2011). Resolving controversies on the path to Alzheimer's therapeutics. *Nat. Med.* 17, 1060–1065. doi:10.1038/nm.2460
- Selwood, S. P., Parvathy, S., Cordell, B., Ryan, H. S., Oshidari, F., Vincent, V., et al. (2009). Gene expression profile of the PDAPP mouse model for Alzheimer's disease with and without apolipoprotein E. *Neurobiol. Aging* 30, 574–590. doi:10.1016/j.neurobiolaging.2007.08.006
- Shen, Y., Lue, L., Yang, L., Roher, A., Kuo, Y., Strohmeier, R., et al. (2001). Complement activation by neurofibrillary tangles in Alzheimer's disease. *Neurosci. Lett.* 305, 165–168. doi:10.1016/S0304-3940(01)01842-0
- Shukla, V., Skuntz, S., and Pant, H. C. (2012). Deregulated Cdk5 activity is involved in inducing Alzheimer's disease. *Arch. Med. Res.* 43, 655–662. doi:10.1016/j.arcmed.2012.10.015
- Snyder, S. E., and Salton, S. R. (1998). Expression of VGF mRNA in the adult rat central nervous system. *J. Comp. Neurol.* 394, 91–105. doi:10.1002/(SICI)1096-9861(19980427)394:1<91::AID-CNE7>3.3.CO;2-B
- Stein, T. D., and Johnson, J. A. (2002). Lack of neurodegeneration in transgenic mice overexpressing mutant amyloid precursor protein is associated with increased levels of transthyretin and the activation of cell survival pathways. *J. Neurosci.* 22, 7380–7388.

- Stover, K. R., and Brown, R. E. (2012). Age-related changes in visual acuity, learning and memory in the APP^{swe}/PS1^{dE9} mouse model of Alzheimer's disease. *Behav. Brain Res.* 231, 75–85. doi:10.1016/j.bbr.2012.02.044
- Südhof, T. C. (1990). The structure of the human synapsin I gene and protein. *J. Biol. Chem.* 265, 7849–7852.
- Sultan, M., Schulz, M. H., Richard, H., Magen, A., Klingenhoff, A., Scherf, M., et al. (2008). A global view of gene activity and alternative splicing by deep sequencing of the human transcriptome. *Science* 321, 956–960. doi:10.1126/science.1160342
- Sutherland, G. T., Janitz, M., and Kril, J. J. (2011). Understanding the pathogenesis of Alzheimer's disease: will RNA-Seq realize the promise of transcriptomics? *J. Neurochem.* 116, 937–946. doi:10.1111/j.1471-4159.2010.07157.x
- Takemura, R., Nakata, T., Okada, Y., Yamazaki, H., Zhang, Z., and Hirokawa, N. (1996). mRNA expression of KIF1A, KIF1B, KIF2, KIF3A, KIF3B, KIF4, KIF5, and cytoplasmic dynein during axonal regeneration. *J. Neurosci.* 16, 31–35.
- Tan, T. C., Valova, V. A., Malladi, C. S., Graham, M. E., Berven, L. A., Jupp, O. J., et al. (2003). Cdk5 is essential for synaptic vesicle endocytosis. *Nat. Cell Biol.* 5, 701–710. doi:10.1038/ncb1020
- Thakker-Varia, S., and Alder, J. (2009). Neuropeptides in depression: role of VGF. *Behav. Brain Res.* 197, 262–278. doi:10.1016/j.bbr.2008.10.006
- Twine, N. A., Janitz, K., Wilkins, M. R., and Janitz, M. (2011). Whole transcriptome sequencing reveals gene expression and splicing differences in brain regions affected by Alzheimer's disease. *PLoS ONE* 6:e16266. doi:10.1371/journal.pone.0016266
- Upadhaya, R. A., Scheibe, F., Kosterin, I., Abramowski, D., Gerth, J., Kumar, S., et al. (2013). The type of A β -related neuronal degeneration differs between amyloid precursor protein (APP23) and amyloid β -peptide (APP48) transgenic mice. *Acta Neuropathol. Commun.* 1, 77. doi:10.1186/2051-5960-1-77
- van Bakel, H., Nislow, C., Blencowe, B. J., and Hughes, T. R. (2010). Most “dark matter” transcripts are associated with known genes. *PLoS Biol.* 8:e1000371. doi:10.1371/journal.pbio.1000371
- van den Pol, A. N., Bina, K., Decavel, C., and Ghosh, P. (1994). VGF expression in the brain. *J. Comp. Neurol.* 347, 455–469. doi:10.1002/cne.903470311
- Verwer, R. W. H., Sluiter, A. A., Balesar, R. A., Baayen, J. C., Noske, D. P., Dirven, C. M. F., et al. (2007). Mature astrocytes in the adult human neocortex express the early neuronal marker doublecortin. *Brain* 130, 3321–3335. doi:10.1093/brain/awm264
- Vogel, C., and Marcotte, E. M. (2012). Insights into the regulation of protein abundance from proteomic and transcriptomic analyses. *Nat. Rev. Genet.* 13, 227–232. doi:10.1038/nrg3185
- Wang, C., Sun, B., Zhou, Y., Grubb, A., and Gan, L. (2012). Cathepsin B degrades amyloid- β in mice expressing wild-type human amyloid precursor protein. *J. Biol. Chem.* 287, 39834–39841. doi:10.1074/jbc.M112.371641
- Wang, Z., Gerstein, M., and Snyder, M. (2009). RNA-Seq: a revolutionary tool for transcriptomics. *Nat. Rev. Genet.* 10, 57–63. doi:10.1038/nrg2484
- Watt, N. T., Whitehouse, I. J., and Hooper, N. M. (2010). The role of zinc in Alzheimer's disease. *Int. J. Alzheimers Dis.* 2011, 971021. doi:10.4061/2011/971021
- Wirhth, O., and Bayer, T. A. (2012). Intraneuronal A β accumulation and neurodegeneration: lessons from transgenic models. *Life Sci.* 91, 1148–1152. doi:10.1016/j.lfs.2012.02.001
- Wirhth, O., Multhaup, G., and Bayer, T. A. (2004). A modified beta-amyloid hypothesis: intraneuronal accumulation of the beta-amyloid peptide – the first step of a fatal cascade. *J. Neurochem.* 91, 513–520. doi:10.1111/j.1471-4159.2004.02737.x
- Wirz, K. T. S., Bossers, K., Stargardt, A., Kamphuis, W., Swaab, D. F., Hol, E. M., et al. (2013). Cortical beta amyloid protein triggers an immune response, but no synaptic changes in the APP^{swe}/PS1^{dE9} Alzheimer's disease mouse model. *Neurobiol. Aging* 34, 1328–1342. doi:10.1016/j.neurobiolaging.2012.11.008
- Wittnam, J. L., Portelius, E., Zetterberg, H., Gustavsson, M. K., Schilling, S., Koch, B., et al. (2012). Pyroglutamate amyloid β (A β) aggravates behavioral deficits in transgenic amyloid mouse model for Alzheimer disease. *J. Biol. Chem.* 287, 8154–8162. doi:10.1074/jbc.M111.308601
- Wu, Z.-L., Ciallella, J. R., Flood, D. G., O'Kane, T. M., Bozyczko-Coyne, D., and Savage, M. J. (2006). Comparative analysis of cortical gene expression in mouse models of Alzheimer's disease. *Neurobiol. Aging* 27, 377–386. doi:10.1016/j.neurobiolaging.2005.02.010
- Yahata, N., Asai, M., Kitaoka, S., Takahashi, K., Asaka, I., Hioki, H., et al. (2011). Anti-A β drug screening platform using human iPS cell-derived neurons for the treatment of Alzheimer's disease. *PLoS ONE* 6:e25788. doi:10.1371/journal.pone.0025788
- Yu, J.-T., and Tan, L. (2012). The role of clusterin in Alzheimer's disease: pathways, pathogenesis, and therapy. *Mol. Neurobiol.* 45, 314–326. doi:10.1007/s12035-012-8237-1

Conflict of Interest Statement: The Tg4–42 mouse model is subject to a patent application by the University Medicine Goettingen.

Received: 17 March 2014; accepted: 02 April 2014; published online: 16 April 2014.

Citation: Bouter Y, Kacprowski T, Weissmann R, Dietrich K, Borgers H, Brauß A, Sperling C, Wirhth O, Albrecht M, Jensen LR, Kuss AW and Bayer TA (2014) Deciphering the molecular profile of plaques, memory decline and neuron loss in two mouse models for Alzheimer's disease by deep sequencing. *Front. Aging Neurosci.* 6:75. doi: 10.3389/fnagi.2014.00075

This article was submitted to the journal *Frontiers in Aging Neuroscience*.

Copyright © 2014 Bouter, Kacprowski, Weissmann, Dietrich, Borgers, Brauß, Sperling, Wirhth, Albrecht, Jensen, Kuss and Bayer. This is an open-access article distributed under the terms of the Creative Commons Attribution License (CC BY). The use, distribution or reproduction in other forums is permitted, provided the original author(s) or licensor are credited and that the original publication in this journal is cited, in accordance with accepted academic practice. No use, distribution or reproduction is permitted which does not comply with these terms.